

Beyond Maximum Likelihood: Variational Inequality Estimation for Generalized Linear Models

Linglingzhi Zhu^{*1}, Jonghyeok Lee^{†1}, and Yao Xie^{‡1}

¹H. Milton Stewart School of Industrial and Systems Engineering
Georgia Institute of Technology

March 3, 2026

Abstract

Generalized linear models (GLMs) are fundamental tools for statistical modeling, with maximum likelihood estimation (MLE) serving as the classical approach for parameter inference. While MLE performs well for canonical GLMs, it can become computationally challenging in more general settings with non-canonical, non-smooth, or nonlinear link functions, where the resulting optimization landscape may be ill-conditioned, non-convex, or non-differentiable. In this paper, we study an alternative estimation framework based on variational inequalities (VIs), which formulates GLM estimation through an operator-based equilibrium condition rather than likelihood minimization. We analyze the VI estimator from a statistical perspective and establish finite-sample error bounds and asymptotic normality under mild regularity conditions, together with convergence guarantees for fixed-point and stochastic approximation algorithms. The framework accommodates a broad class of link functions, including non-canonical and non-monotone cases satisfying a strong Minty-type condition, and extends naturally to generalized additive models via basis expansion. Numerical experiments demonstrate that the VI approach achieves competitive finite-sample accuracy and improved numerical stability relative to MLE, particularly in GLMs and GAMs with non-canonical or non-smooth link functions.

1 Introduction

Generalized linear models (GLMs) are a cornerstone of statistics and machine learning, providing a unified framework that extends linear regression to accommodate diverse response types through the exponential-family formulation [17, 16]. By linking the conditional mean of the response to a linear predictor via a specified link function, GLMs combine interpretability and flexibility, encompassing classical models such as linear, logistic, and Poisson regression as special cases. Owing to this balance, GLMs have been widely used across scientific, engineering, and data-driven decision-making domains.

The central inferential task in GLMs is to estimate the regression parameter characterizing the relationship between covariates and responses. Maximum likelihood estimation (MLE) has long served as the canonical approach, offering strong asymptotic guarantees such as consistency and

^{*}lzzhu@gatech.edu

[†]jlee4177@gatech.edu

[‡]yao.xie@isye.gatech.edu

efficiency under correct model specification. However, in modern modeling scenarios, MLE can face substantial computational challenges. When the link function departs from the canonical form or incorporates non-smooth or nonlinear structures designed for robustness and flexibility, the resulting likelihood-based objective may become ill-conditioned, non-convex, or non-differentiable. These issues often lead to slow convergence, sensitivity to initialization, and numerical instability, particularly in high-dimensional settings. Such difficulties motivate alternative formulations that retain the interpretability of GLMs while improving computational behavior and theoretical robustness.

In this paper, we study *variational inequality (VI)-based estimation* as a principled alternative to MLE for GLMs. The VI framework, originally proposed by Juditsky and Nemirovski [8] for nonlinear least-squares problems, provides an operator-based formulation of estimation defined through an equilibrium condition rather than likelihood minimization. This perspective naturally accommodates non-canonical and even non-monotone link functions, relaxing the smoothness and convexity requirements inherent in likelihood-based approaches. It also enables a unified treatment of statistical accuracy and algorithmic convergence within a single framework.

Contributions. Our analysis shows that the VI formulation recovers the MLE first-order optimality condition under canonical links and yields a novel moment-based estimator for non-canonical links that can improve numerical performance. We establish key statistical guarantees for the VI estimator, including $\mathcal{O}(N^{-1/2})$ consistency and asymptotic normality with a sandwich-type covariance structure. On the computational side, we provide convergence guarantees for fixed-point and stochastic approximation algorithms used to compute the estimator. The framework accommodates non-canonical, non-smooth, and even non-monotone link functions under a mild Minty-type condition. It also extends naturally to generalized additive models (GAMs) via basis expansion. Empirically, the VI estimator achieves improved numerical stability and faster convergence relative to MLE in challenging GLM and GAM settings.

Viewed more broadly, this formulation reflects a decision-centric perspective on estimation, in which estimators are designed around operator geometry that supports stable computation and inference, rather than around likelihood curvature alone.

2 Background and Problem Setup

We briefly review the generalized linear model (GLM) framework and establish notation used throughout the paper. We then describe maximum likelihood estimation (MLE) and its reformulation as a variational inequality (VI), which forms the basis of our analysis. A summary of notation is provided in Appendix A.

Given i.i.d. samples (\mathbf{x}, y) , where $\mathbf{x} \in \mathbb{R}^d$ denotes the covariates and $y \in \mathbb{R}$ the response, a GLM specifies the conditional distribution of $y \mid \mathbf{x}$ using the exponential family. The conditional mean is linked to a linear predictor through a link function $g : \mathbb{R} \rightarrow \mathbb{R}$:

$$\mathbb{E}[y \mid \mathbf{x}] = g^{-1} \left(\beta_0 + \sum_{j=1}^d \beta_j x_j \right), \quad (2.1)$$

where $\boldsymbol{\beta} = (\beta_0, \dots, \beta_d) \in \mathbb{R}^{d+1}$ is the coefficient vector including an intercept. Classical examples include logistic regression with a binomial distribution and logit link, and Poisson regression with a Poisson distribution and logarithmic link.

Maximum likelihood estimation. A standard approach for estimating β is maximum likelihood estimation (MLE). Given a model with density (or mass) function $p(y; \beta)$ and observations $\{y^i\}_{i=1}^N$, the MLE minimizes the empirical negative log-likelihood (NLL),

$$\min_{\beta \in \mathbb{R}^{d+1}} \mathcal{L}_N(\beta) := \sum_{i=1}^N \ell \left(g^{-1} \left(\beta_0 + \sum_{j=1}^d \beta_j x_j^i \right), y^i \right). \quad (\text{MLE})$$

Problem (MLE) can be solved using second-order methods such as Fisher scoring or IRLS [4, 16], as well as first-order or stochastic methods in large-scale settings [18, 14].

When canonical link functions are used, (MLE) is convex and smooth, ensuring global optimality and efficient convergence. In contrast, for non-canonical links the optimization landscape can become ill-conditioned, leading to slow convergence or numerical instability [6]. Moreover, when the inverse link function is non-smooth or saturating, as in Poisson regression with clipped intensity functions [2] or models using piecewise-linear activations such as hinge or ReLU functions, the resulting NLL objective may be non-convex or non-differentiable. These features motivate alternative formulations that do not rely on smooth, well-conditioned likelihood landscapes.

Variational inequality formulation. We reformulate estimation as a variational inequality. Let $V : \mathbb{R}^{d+1} \rightarrow \mathbb{R}^{d+1}$ denote the population operator

$$V(\beta) := \mathbb{E}_{(\mathbf{x}, y) \sim \mathbb{P}} \left[\left(g^{-1} \left(\beta_0 + \sum_{j=1}^d \beta_j x_j \right) - y \right) \tilde{\mathbf{x}} \right],$$

where $\tilde{\mathbf{x}} := [1; \mathbf{x}] \in \mathbb{R}^{d+1}$. We define the target parameter β^* as the solution to the population variational inequality

$$\langle V(\beta^*), \beta - \beta^* \rangle \geq 0, \quad \forall \beta \in \mathbb{R}^{d+1}. \quad (2.2)$$

When a canonical link is used, this condition coincides with the population first-order optimality condition of the MLE, and β^* equals the population MLE. For non-canonical links, (2.2) defines a moment-based target parameter characterized by the conditional mean relationship (2.1), independently of the likelihood geometry.

Given samples $\{(\mathbf{x}^i, y^i)\}_{i=1}^N$, the empirical VI estimator $\hat{\beta}_N$ is defined as

$$\hat{\beta}_N \in \left\{ \hat{\beta} \in \mathbb{R}^{d+1} : \langle V_N(\hat{\beta}), \beta - \hat{\beta} \rangle \geq 0, \forall \beta \in \mathbb{R}^{d+1} \right\}, \quad (\text{VI})$$

with

$$V_N(\beta) := \frac{1}{N} \sum_{i=1}^N \left(g^{-1}(\tilde{\mathbf{x}}^{i\top} \beta) - y^i \right) \tilde{\mathbf{x}}^i.$$

Relation to prior work. The VI formulation generalizes the MLE score equation in the sense that, under canonical links, the gradient of the NLL coincides exactly with the operator $V_N(\beta)$. This operator-based perspective was introduced by Juditsky and Nemirovski [8] and builds on earlier perceptron-type methods [20, 12, 11]. Subsequent work has extended VI-based estimation to online and stochastic settings and to monotone or weakly monotone link functions [9, 10, 3, 23, 15].

In contrast to existing analyses that focus primarily on stochastic approximation schemes, our work studies the sample-average VI estimator as a statistical object. We establish finite-sample estimation error bounds, asymptotic normality, and explicit convergence guarantees for deterministic and stochastic algorithms. Compared to likelihood-based formulations, the VI approach enables stable computation under weaker smoothness assumptions on the link function, at the cost of a potential loss of asymptotic efficiency in non-canonical settings.

2.1 Summary of main results

We summarize the main theoretical and algorithmic results for VI-based estimation in GLMs. Our analysis assumes a Lipschitz inverse link and a strong Minty-type condition on the associated VI operator, under which both statistical consistency and algorithmic convergence can be established. Section 4 proves finite-sample and asymptotic properties of the empirical VI solution, including a high-probability estimation error bound of order $\tilde{O}(\sqrt{d/N})$ and asymptotic normality with a sandwich-type covariance matrix. Section 5 analyzes algorithms for computing the VI estimator, showing linear convergence of a fixed-point iteration under the strong Minty condition and standard sublinear rates for stochastic approximation in the streaming data setting. The results apply to non-canonical links, including non-smooth and potentially non-monotone inverse links satisfying the strong Minty condition (e.g., clipped and ReLU-type links); under canonical links, the VI formulation reduces to the first-order optimality condition of the MLE.

3 From MLE to VI

We consider the GLM defined in (2.1), where the response follows an exponential-family distribution with mean $g^{-1}(\tilde{\mathbf{x}}^\top \boldsymbol{\beta})$. The choice of the loss ℓ and inverse link g^{-1} significantly impacts the optimization landscape.

Why MLE optimization can fail for general link functions. Next, we show that MLE optimization can become difficult when the inverse link introduces non-convex or non-smooth structure. Consider the two-sided clipped exponential link

$$g^{-1}(z) = \max\{c, \min\{e^z, C\}\}, \quad 0 < c < C,$$

and the Poisson negative log-likelihood

$$(\ell \circ g^{-1})(z) = -y \log(g^{-1}(z)) + g^{-1}(z).$$

This composition is piecewise smooth with flat regions for $z \leq \log c$ and $z \geq \log C$, and is non-differentiable at the two kink points. A direct inspection of the one-sided derivatives shows that the monotonicity conditions required for convexity cannot hold simultaneously when $0 < c < C$. Hence, $\ell \circ g^{-1}$ is globally non-convex and non-smooth.

For illustration, letting $y = 1$ and $x = 1$ yields

$$\mathcal{L}(\beta) = -\log g^{-1}(\beta) + g^{-1}(\beta).$$

As shown in Figures 1(a) and (b), clipping induces wide flat plateaus where gradient-based MLE updates can stall and fail to reach the global minimizer at $\beta = 0$. In contrast, Figure 1(c) shows that the corresponding VI vector field remains monotone, so simple fixed-point iterations can still converge to the global solution.

Equivalence under canonical links. When the model employs a canonical link function (e.g., Logit for Logistic, Identity for Normal), the gradient of the NLL coincides exactly with the VI operator:

$$\nabla \mathcal{L}_N(\boldsymbol{\beta}) = V_N(\boldsymbol{\beta}).$$

This implies that MLE and VI share identical first-order optimality conditions. Representative examples are summarized in Table 1. However, for non-canonical links, this equivalence breaks, and MLE often suffers from optimization challenges.

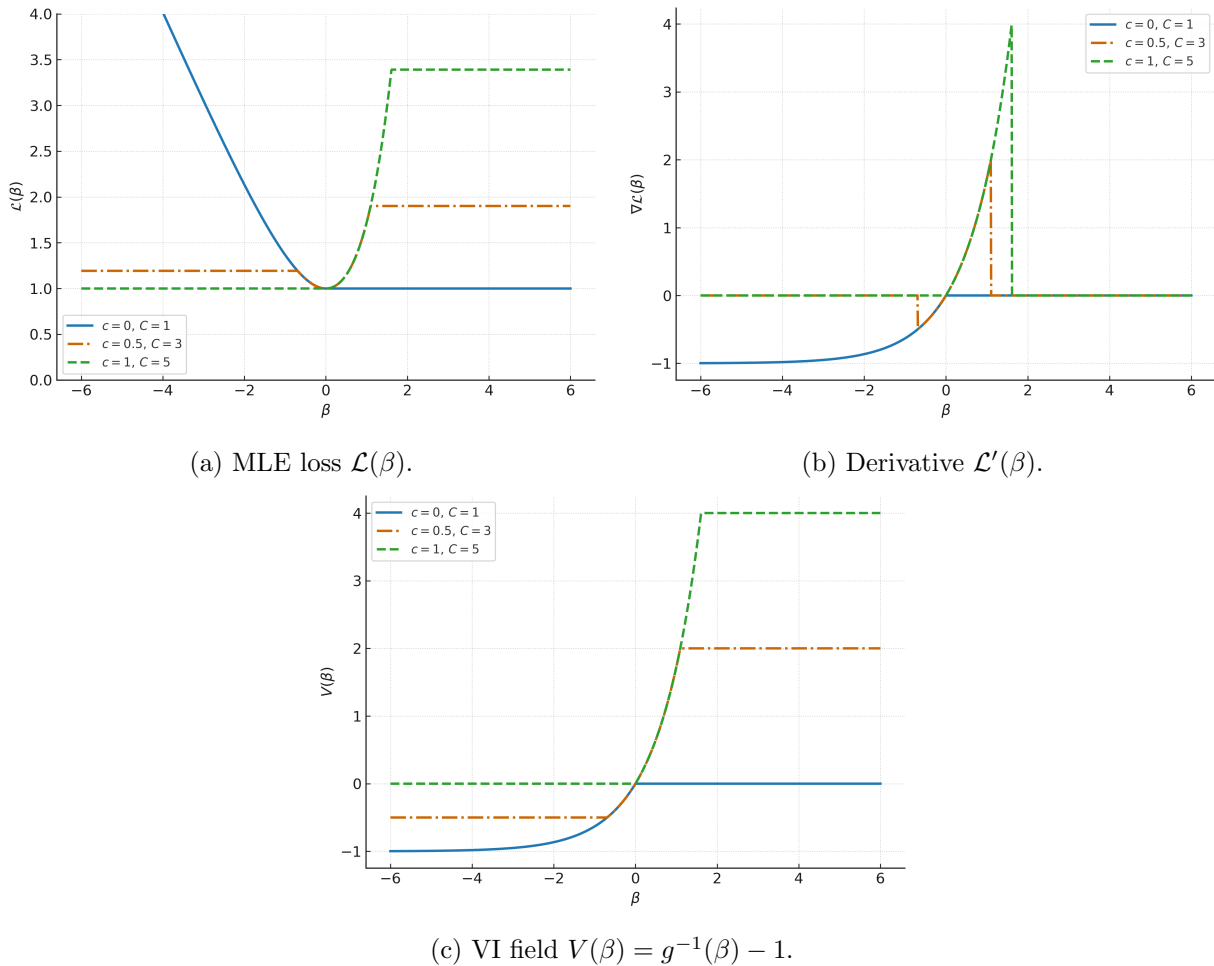


Figure 1: Clipped exponential link: MLE loss, its derivative, and the VI vector field.

Flatness of MLE landscape. It is well known that MLE optimization algorithms can converge slowly near the true parameter, especially in the non-canonical settings when the likelihood surface is nearly flat or ill-conditioned. Consider the softplus link $g^{-1}(z) = \log(1 + e^z)$ in Poisson regression. In this case, the Hessian of the MLE objective decays rapidly in the right tail (as $z \rightarrow \infty$). In contrast, the Jacobian of the VI operator remains well-conditioned. This flatness in MLE leads to weaker local contraction and slower convergence compared to VI.

Non-convexity and Non-smoothness. More severe issues arise with robust or truncated links. For instance, with the two-sided clipped exponential link $g^{-1}(z) = \max\{c, \min\{e^z, C\}\}$, the composition of the NLL loss for Poisson regression and the link results in a globally non-convex and non-smooth objective. The MLE loss exhibits flat plateaus with zero gradients, causing gradient-based methods to get stuck. Conversely, the VI vector field remains monotone, ensuring that standard iterative solvers can still recover the global solution.

Detailed derivations and landscape visualizations are provided in Appendix B.

Table 1: MLE and VI Formulations under Different Links.

Model	Loss $\ell(u, y)$	Inverse Link $g^{-1}(z)$	Equiv?
Logistic	$-y \log u - (1 - y) \log(1 - u)$	$e^z / (1 + e^z)$	✓
		$\frac{1}{2} + \frac{1}{\pi} \arctan(z)$	✗
Normal	$\frac{1}{2}(u - y)^2$	z	✓
		$\max\{0, z\}$	✗
Exp.	$\log u + y/u$	z^{-1}	✓
		e^{-z}	✗
Poisson	$-y \log u + u$	e^z	✓
		$\log(1 + e^z)$	✗
		$\max\{c, \min\{e^z, C\}\}$	✗

4 Statistical Guarantees of VI Estimators

Having established the formulation in (VI) and its motivation, we now turn to the theoretical analysis of the proposed estimator’s statistical properties. This section derives both finite-sample and asymptotic guarantees for the empirical VI solution, defined as

$$\hat{\beta}_N \in \text{Sol}(V_N),$$

i.e., $V_N(\hat{\beta}_N) = \sum_{i=1}^N (g^{-1}(\tilde{\mathbf{x}}^{i\top} \hat{\beta}_N) - y^i) \tilde{\mathbf{x}}^i = \mathbf{0}$. We begin with the following assumptions, which are used throughout the paper:

Assumption 4.1.

- (i) *The inverse link function g^{-1} is L -Lipschitz continuous.*
- (ii) *The true parameter β^* and all the data (\mathbf{x}, y) satisfy*

$$\left| g^{-1}(\tilde{\mathbf{x}}^\top \beta^*) - y \right| \leq R.$$

- (iii) *The feature vector \mathbf{x} satisfies $|x_j| \leq M$ and $|x_j \cdot y| \leq M$ for all $j \in [d]$ and all (\mathbf{x}, y) .*
- (iv) *The population operator V and the empirical operator V_N satisfy the strong Minty condition with modulus $\mu > 0$ for any $\beta \in \mathbb{R}^{d+1}$:*

$$\langle V(\beta), \beta - \beta^* \rangle \geq \mu \|\beta - \beta^*\|^2, \quad \langle V_N(\beta), \beta - \hat{\beta}_N \rangle \geq \mu \|\beta - \hat{\beta}_N\|^2.$$

Consequently, the solution sets $\text{Sol}(V)$ and $\text{Sol}(V_N)$ are nonempty and singleton.

Remark 4.1 (Strong Minty condition). The strong Minty condition is a relatively mild regularity requirement compared to strong monotonicity. In Assumption 4.1, we adopt a slightly stronger version to ensure the uniqueness of both the true parameter β^* and the sample-averaged solution $\hat{\beta}_N$ for simplicity. Nevertheless, this assumption can be relaxed to the standard projection-based form in Definition C.1, by replacing β^* and $\hat{\beta}_N$ with $\text{proj}_{\text{Sol}(V)}(\beta)$ and $\text{proj}_{\text{Sol}(V_N)}(\beta)$, respectively. Intuitively, it requires that the vector field F exhibits at least linear growth away from the solution,

with a uniform positive coefficient that prevents flat or degenerate regions around the solution. Geometrically, in the one-dimensional case, this means that F defines a supporting hyperplane at the solution that strictly separates the solution from all other points, thereby ensuring the local stability of the solution. Further discussion and sufficient conditions are provided in Appendix C; see also related treatments in [7].

With these preparations in place, we now proceed to derive finite-sample estimation error bounds that characterize the deviation between the empirical solution $\hat{\beta}_N$ and the population parameter β^* in Section 4.1. We then establish that the VI estimator is $\mathcal{O}(N^{-1/2})$ -consistent and asymptotically normal, exhibiting a sandwich-type covariance structure analogous to that of the MLE, as detailed in Section 4.2.

4.1 Finite-sample estimation error

As a first step, we establish the following auxiliary lemma. Associated with the pair (\mathbf{x}, y) , we recall the vector field $V_{(\mathbf{x}, y)} : \mathbb{R}^{d+1} \rightarrow \mathbb{R}^{d+1}$

$$V_{(\mathbf{x}, y)}(\beta) := \left(g^{-1} \left(\tilde{\mathbf{x}}^\top \beta \right) - y \right) \tilde{\mathbf{x}}.$$

Now, we are ready to derive the following estimation error of the variational inequality (VI).

Theorem 4.1 (Estimation error). *Suppose that Assumption 4.1 holds. Then for any $\epsilon \in (0, 1)$, with the probability at least $1 - \epsilon$, we have the following estimation error*

$$\|\hat{\beta}_N - \beta^*\| \leq \frac{RM}{\mu} \sqrt{\frac{2(d+1) \ln(2(d+1)/\epsilon)}{N}}.$$

Remark 4.2. For the MLE, a similar finite-sample error bound can be derived as $\tilde{\mathcal{O}}(\sqrt{d}/(\mu' \sqrt{N}))$, where $\mu' > 0$ denotes the curvature modulus of the composite mapping $\ell \circ g^{-1}$ that satisfies the restricted secant inequality (RSI), i.e., for the maximum likelihood estimator $\bar{\beta}_N$ and any β

$$\langle \nabla \mathcal{L}_N(\beta), \beta - \bar{\beta}_N \rangle \geq \mu' \|\beta - \bar{\beta}_N\|^2,$$

a condition stronger than the Polyak–Łojasiewicz inequality and weaker than the strong convexity; see [13]. Recall that the gradient of the empirical loss of (MLE) is given by

$$\nabla \mathcal{L}_N(\beta) = \mathbb{E}_{(\mathbf{x}, y) \sim \mathbb{P}_N} \left[(g^{-1})' \left(\tilde{\mathbf{x}}^\top \beta \right) \ell' \left(g^{-1} \left(\tilde{\mathbf{x}}^\top \beta \right), y \right) \tilde{\mathbf{x}} \right].$$

If the RSI holds with constant μ' , then

$$\mu' \|\bar{\beta}_N - \beta^*\|^2 \leq \langle \nabla \mathcal{L}_N(\beta^*), \beta^* - \bar{\beta}_N \rangle,$$

which implies the bound

$$\|\bar{\beta}_N - \beta^*\| \leq \frac{\|\nabla \mathcal{L}_N(\beta^*)\|}{\mu'}.$$

Compared with the proof of the VI estimator in Theorem 4.1, where g^{-1} itself satisfies the strong Minty condition, the MLE requires the composite operator $(\ell' \circ g^{-1}) \cdot (g^{-1})'$ to satisfy an analogous Minty-type condition. This composite structure makes the regularity requirement for MLE substantially more intricate.

4.2 Asymptotic normality of VI estimators

We now proceed to establish the asymptotic normality of the VI estimator. Our goal is to show that $\sqrt{N}(\hat{\beta}_N - \beta^*)$ converges in distribution to a normal random vector with mean zero and a sandwich-type covariance matrix. To handle potential nonsmoothness of the link function g^{-1} , we employ tools from empirical process theory and a local linearization argument around the population solution β^* .

Since g^{-1} is globally Lipschitz by Assumption 4.1, Rademacher's theorem [19, Theorem 9.60] implies that it is differentiable almost everywhere on \mathbb{R} , and hence its nondifferentiability set

$$\mathcal{K} := \{t : (g^{-1})'(t) \text{ does not exist}\}$$

has Lebesgue measure zero. We further assume the following condition.

Assumption 4.2. *The random variable $\langle \tilde{\mathbf{x}}, \beta^* \rangle$ does not fall on the nondifferentiability set \mathcal{K} of g^{-1} , that is,*

$$\mathbb{P}(\langle \tilde{\mathbf{x}}, \beta^* \rangle \in \mathcal{K}) = 0.$$

This assumption is not restrictive in practice, since \mathcal{K} has Lebesgue measure zero and thus the event $\langle \tilde{\mathbf{x}}, \beta^* \rangle \in \mathcal{K}$ occurs with probability zero for any continuous feature distribution. With this mild condition, the population VI operator V is guaranteed to be differentiable at the true parameter β^* .

Lemma 4.2. *Suppose that Assumptions 4.1 and 4.2 hold. Then the function V is Fréchet differentiable at β^* with its Jacobian*

$$\nabla V(\beta^*) = \mathbb{E}_{(\mathbf{x}, y) \sim \mathbb{P}} \left[(g^{-1})'(\langle \tilde{\mathbf{x}}, \beta^* \rangle) \tilde{\mathbf{x}} \tilde{\mathbf{x}}^\top \right].$$

Owing to the averaging-induced smoothing effect, we obtain the asymptotic normality result.

Theorem 4.3 (Asymptotic normality of the VI estimator). *Suppose Assumptions 4.1 and 4.2 hold, and in addition*

(A1) *The Jacobian $\nabla V(\beta^*)$ is non-singular.*

(A2) *The covariance matrix*

$$\Gamma := \mathbb{E}_{(\mathbf{x}, y) \sim \mathbb{P}} [V_{(\mathbf{x}, y)}(\beta^*) V_{(\mathbf{x}, y)}(\beta^*)^\top] = \mathbb{E}_{(\mathbf{x}, y) \sim \mathbb{P}} [(y - g^{-1}(\tilde{\mathbf{x}}^\top \beta^*))^2 \tilde{\mathbf{x}} \tilde{\mathbf{x}}^\top]$$

is finite and positive definite.

Then $\hat{\beta}_N$ is \sqrt{N} -consistent and

$$\sqrt{N}(\hat{\beta}_N - \beta^*) \xrightarrow{d} \mathcal{N}(0, \nabla V(\beta^*)^{-1} \Gamma \nabla V(\beta^*)^{-\top}).$$

The resulting asymptotic covariance exhibits a sandwich structure analogous to that of the MLE. While the MLE attains the Cramér-Rao lower bound under correctly specified models, the slight difference in asymptotic efficiency for the VI estimator represents a necessary trade-off for the superior computational stability and global convergence guarantees it offers in non-canonical settings. We provide a detailed efficiency comparison in Appendix E.

5 Convergence of VI-Based Algorithms

This section investigates the computational efficiency of solving the empirical VI problem using iterative algorithms. We begin by analyzing the convergence behavior of a fixed-point iterative method under a fixed sample size N . We then extend the analysis to the stochastic approximation setting, where the estimation is performed using a streaming data scheme.

For the following deterministic fixed-point iterative scheme under a fixed sample size, we establish its linear convergence rates under the strong Minty condition.

Algorithm 1: Fixed-Point Iterative Method

Input: Initialization β^0 , step size $\eta > 0$, data $(\mathbf{x}, y) \sim \mathbb{P}_N$

- 1 **for** $t = 0, 1, 2, \dots, T - 1$ **do**
- 2 | $\beta^{t+1} := \beta^t - \eta \cdot V_N(\beta^t)$
- 3 **end**

Theorem 5.1 (Linear convergence of fixed-point method). *Suppose that Assumption 4.1 holds with the step size*

$$\eta = \frac{\mu}{L^2(1 + dM^2)^2},$$

where $\mu > 0$ is the strong Minty modulus in Assumption 4.1. Then the sequence of estimates β^t given by the Algorithm 1 for every $t = 0, 1, 2, \dots$ satisfies

$$\|\beta^t - \hat{\beta}_N\|^2 \leq \left(1 - \frac{\mu^2}{L^2(1 + dM^2)^2}\right)^t \cdot \|\beta^0 - \hat{\beta}_N\|^2,$$

Furthermore, for any $\epsilon \in (0, 1)$, with the probability at least $1 - \epsilon$, we have the following estimation error

$$\|\beta^t - \beta^*\| \leq \left(1 - \frac{\mu^2}{L^2(1 + dM^2)^2}\right)^{t/2} \cdot \|\beta^0 - \hat{\beta}_N\| + \frac{RM}{\mu} \sqrt{\frac{2(d+1) \ln(2(d+1)/\epsilon)}{N}}.$$

Next, we consider the stochastic approximation setting, in which the estimator is updated from streaming data.

Algorithm 2: Stochastic Approximation

Input: Initialization β^0 , step size $\eta^t > 0$, streaming data $(\mathbf{x}^t, y^t) \sim \mathbb{P}$

- 1 **for** $t = 0, 1, 2, \dots, T - 1$ **do**
- 2 | $\beta^{t+1} := \beta^t - \eta^t \cdot V_{(\mathbf{x}^t, y^t)}(\beta^t)$
- 3 **end**

Theorem 5.2 (Sublinear estimation error of stochastic approximation). *Suppose that Assumption 4.1 holds. Then the sequence $\{\beta^t\}_{t \geq 0}$ generated by Algorithm 2 with step size*

$$\eta^t = \frac{1}{\mu(t+1)}, \quad t = 0, 1, 2, \dots,$$

where $\mu > 0$ is the strong Minty modulus in Assumption 4.1, satisfies

$$\mathbb{E}\|\beta^t - \beta^*\|^2 \leq \frac{c_0(d+1)R^2M^2}{\mu^2(t+1)}, \quad t = 0, 1, 2, \dots,$$

for some constant $c_0 > 1$ that depends on the initialization.

These results collectively show that the proposed VI-based algorithms achieve both statistical consistency and efficient convergence, even under non-smooth or non-monotone link functions, thereby underscoring the computational advantages of the proposed framework for general estimation problems.

6 Numerical Experiments

We examine the finite-sample performance of the VI estimator relative to the MLE in Poisson regression with various link functions. For each experiment, the true parameter is fixed as $\beta^* = d^{-1/2}(1, \dots, 1) \in \mathbb{R}^d$, and the covariates $\mathbf{x}^i \in \mathbb{R}^d$, $i = 1, \dots, N$, are drawn i.i.d. from $\mathcal{N}(0, I_d)$. Given \mathbf{x}^i , the response $y^i \in \mathbb{R}$ is generated according to

$$y^i \sim \text{Poisson}\left(g^{-1}(\beta^\top \mathbf{x}^i)\right),$$

with no intercept term. We consider the following inverse link functions: (i) the log link $g^{-1}(z) = e^z$; (ii) the softplus link $g^{-1}(z) = \log(1 + e^z)$; (iii) the clipped exponential link $g^{-1}(z) = \min\{e^z, 2\}$; and (iv) a scaled Gaussian-mixture CDF with two components,

$$g^{-1}(z) = 1.65 \Phi\left(\frac{z+0.5}{0.7}\right) + 1.35 \Phi\left(\frac{z-1.2}{0.5}\right),$$

where $\Phi(z) = \int_{-\infty}^z \exp(-x^2/2)/\sqrt{2\pi} dx$ is the standard Gaussian CDF. The log link corresponds to the canonical Poisson model, for which the VI and MLE updates coincide. The softplus and clipped exponential links introduce bounded curvature and truncation in the mean function, respectively, while the Gaussian-mixture CDF provides a non-convex example designed to test robustness in more challenging settings.

For each link, both estimators are computed by iterative updates of the form

$$\beta^{k+1} = \beta^k - \eta^k V(\beta^k),$$

$$\beta^{k+1} = \beta^k - \eta^k \nabla \mathcal{L}(\beta^k),$$

with exponentially decaying step size with base $\eta^0 = 0.01$ scaled by $\sqrt{N/d}$. We consider dimensions $d \in \{10, 20, \dots, 100\}$, sample sizes $N \in \{100, 200, \dots, 1000\}$.

Table 2 reports the average squared error $\|\beta^k - \beta^*\|^2$ over 1000 replications for both VI and MLE after $k \in \{20, 50, 100, 200\}$ iterations using the softplus link function. The VI estimator consistently attains smaller error than MLE at every iteration count, often by a larger margin especially at the early stage. A more comprehensive set of results with other link functions and a sparse parameter setting can be found in Appendix G, where we observe that VI generally dominates MLE, except for the Gaussian-mixture CDF link in the “easy” regime of large sample size, low dimension, and large iterations.

Figure 2 and Figure 3 illustrate representative convergence behavior for $(d, N) = (20, 400)$. Figure 2 shows the sample convergence trajectories of the VI and MLE iterates for all four link functions. The trajectories for the log link coincide exactly, as expected from their equivalence as in Appendix B.1. For non-canonical links, the VI update exhibits noticeably faster convergence in the early iteration phase. In the clipped exponential case, the VI and MLE trajectories coincide during the initial iterations because the iterates have not yet reached the truncation boundary, and the model effectively behaves like the log link in that region. For the Gaussian-mixture CDF link, which induces a highly non-convex regime, VI avoids the oscillations and occasional divergence observed in MLE.

Table 2: Mean squared error of the VI estimator and MLE with softplus link across iterations k . For each (k, d, N) combination, the smaller error between the two estimators is highlighted in bold. The values in the brackets are standard deviations across 1000 independent repetitions.

k	d	$N = 100$		$N = 200$		$N = 500$		$N = 1000$	
		VI	MLE	VI	MLE	VI	MLE	VI	MLE
20	10	.63 (.08)	.71 (.06)	.51 (.07)	.62 (.06)	.34 (.06)	.47 (.05)	.21 (.04)	.34 (.03)
	20	.73 (.07)	.79 (.05)	.63 (.06)	.71 (.05)	.47 (.05)	.58 (.04)	.33 (.04)	.46 (.03)
	50	.82 (.05)	.87 (.03)	.75 (.04)	.81 (.03)	.63 (.04)	.71 (.03)	.51 (.03)	.62 (.03)
	100	.88 (.03)	.91 (.02)	.83 (.03)	.87 (.02)	.73 (.03)	.79 (.02)	.63 (.03)	.71 (.02)
50	10	.47 (.10)	.57 (.09)	.32 (.08)	.44 (.07)	.16 (.05)	.27 (.05)	.08 (.03)	.16 (.03)
	20	.59 (.09)	.67 (.07)	.46 (.07)	.57 (.06)	.28 (.05)	.40 (.05)	.16 (.03)	.27 (.03)
	50	.75 (.06)	.80 (.05)	.64 (.06)	.71 (.05)	.46 (.05)	.57 (.04)	.32 (.04)	.44 (.03)
	100	.83 (.05)	.86 (.04)	.74 (.05)	.79 (.04)	.59 (.04)	.68 (.03)	.46 (.03)	.56 (.03)
100	10	.40 (.11)	.50 (.10)	.26 (.08)	.36 (.08)	.12 (.04)	.20 (.04)	.05 (.02)	.11 (.03)
	20	.54 (.10)	.62 (.08)	.40 (.08)	.50 (.07)	.22 (.05)	.32 (.05)	.12 (.03)	.20 (.03)
	50	.71 (.07)	.76 (.06)	.59 (.06)	.66 (.05)	.40 (.05)	.50 (.04)	.26 (.04)	.36 (.03)
	100	.82 (.05)	.84 (.04)	.72 (.05)	.76 (.04)	.54 (.05)	.63 (.04)	.40 (.04)	.50 (.03)
200	10	.38 (.12)	.48 (.10)	.24 (.08)	.34 (.08)	.10 (.04)	.18 (.04)	.05 (.02)	.09 (.02)
	20	.53 (.11)	.61 (.09)	.38 (.08)	.47 (.07)	.20 (.04)	.30 (.04)	.10 (.03)	.18 (.03)
	50	.71 (.07)	.75 (.06)	.57 (.07)	.64 (.06)	.38 (.05)	.48 (.04)	.24 (.04)	.34 (.03)
	100	.82 (.06)	.84 (.04)	.70 (.06)	.75 (.04)	.52 (.05)	.61 (.04)	.38 (.04)	.48 (.03)

Figure 3 reports the average squared error against the iteration count k . The gap between VI and MLE is particularly pronounced for the softplus link, where VI converges significantly faster. For the clipped exponential link, the gap becomes more pronounced in the later iterations as the iterations approach the truncation boundary. For the Gaussian-mixture CDF link, the gap is largest during the early iterations and gradually narrows as both methods stabilize.

Overall, the results demonstrate that the proposed VI framework achieves comparable estimation accuracy to MLE under finite sample sizes, while often exhibiting faster convergence and greater numerical stability for non-canonical link functions. With canonical links, both methods coincide, but in more general GLMs, the VI formulation effectively mitigates the flat-landscape and conditioning issues that slow gradient-based likelihood estimation.

7 Extension to Generalized Additive Models

Generalized additive models (GAMs) [5] extend GLMs by replacing the linear predictor with an additive (component-wise) structure, while retaining the exponential-family modeling of the response. Suppose we observe i.i.d. pairs (\mathbf{x}, y) , where $\mathbf{x} = (x_1, \dots, x_d) \in \mathbb{R}^d$ is the feature vector and $y \in \mathbb{R}$ is the response. A GAM links the conditional mean to the covariates via

$$\mathbb{E}[y | \mathbf{x}] = g^{-1} \left(\beta_0 + \sum_{j=1}^d f_j(x_j) \right),$$

where g^{-1} is the inverse link function, $\beta_0 \in \mathbb{R}$ is the intercept, and each additive component $f_j : \mathbb{R} \rightarrow \mathbb{R}$ describes the nonlinear effect of the j -th feature. To ensure identifiability, we impose

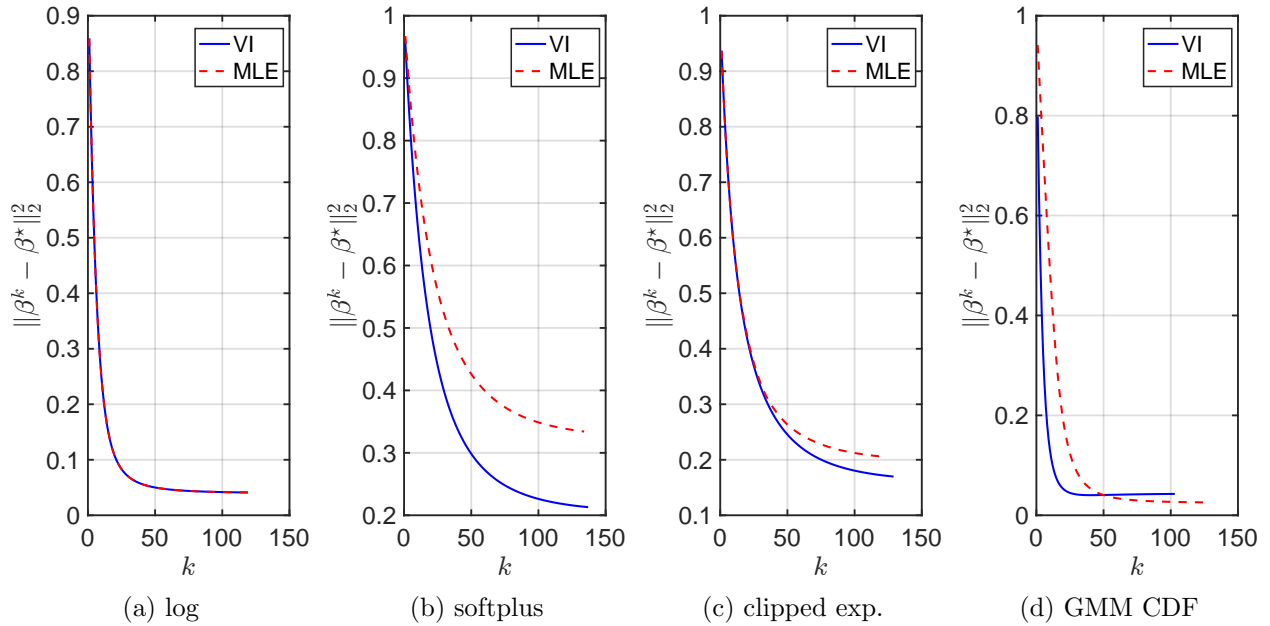


Figure 2: Convergence trajectories of VI and MLE for Poisson regression with different link functions ($d = 20, N = 400$).

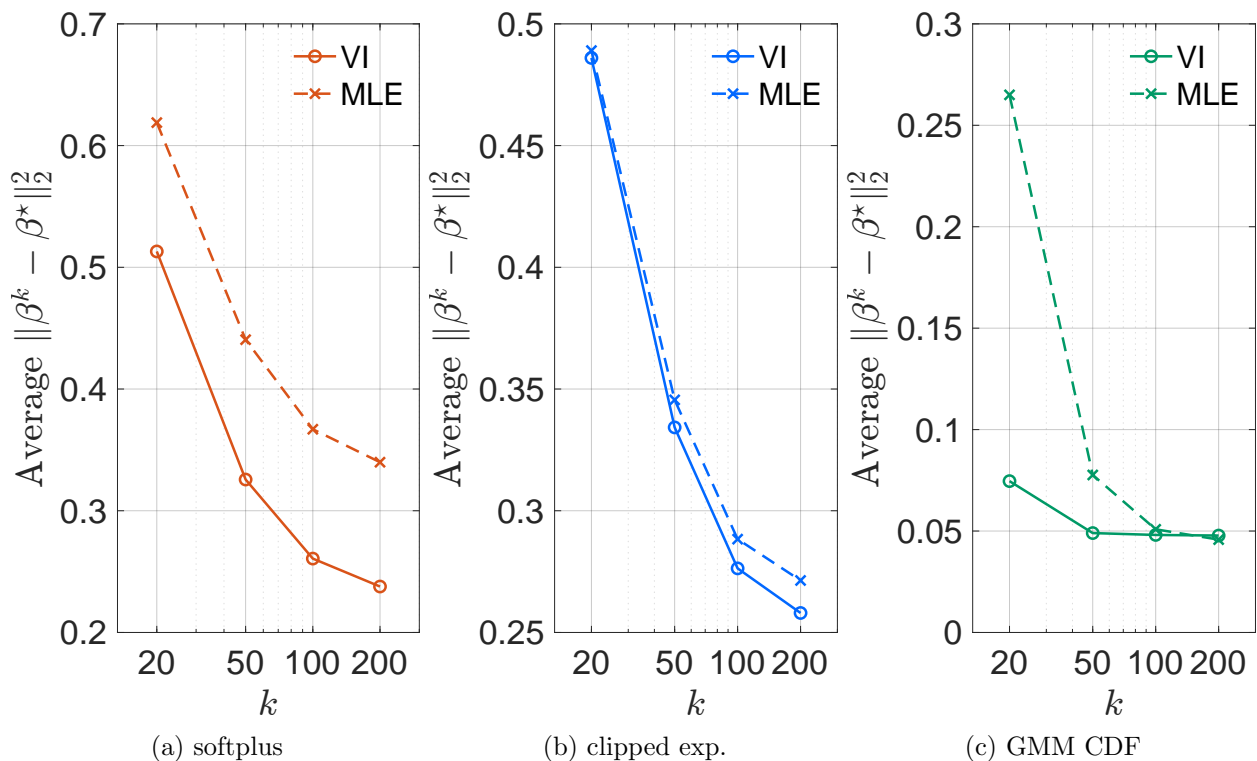


Figure 3: Average squared error for VI and MLE against iteration budgets for Poisson regression with different link functions ($d = 20, N = 400$).

the standard constraint $f_j(0) = 0$ (alternatively one may impose a centering constraint such as $\mathbb{E}[f_j(X_j)] = 0$).

Basis representation. To render the estimation problem finite-dimensional, we approximate each component function f_j using a truncated basis expansion. Let $\{\psi_k\}_{k=1}^K$ be a set of basis functions (e.g., B-splines or polynomials) satisfying $\psi_k(0) = 0$, so that $f_j(0) = 0$ holds automatically. We parameterize

$$f_j(x_j) \approx \sum_{k=1}^K \beta_{jk} \psi_k(x_j), \quad j = 1, \dots, d.$$

Define the stacked feature mapping $\Phi : \mathbb{R}^d \rightarrow \mathbb{R}^{dK}$ by

$$\Phi(\mathbf{x}) := [\psi_1(x_1), \dots, \psi_K(x_1), \dots, \psi_1(x_d), \dots, \psi_K(x_d)]^\top,$$

and $\tilde{\Phi}(\mathbf{x}) := [1; \Phi(\mathbf{x})] \in \mathbb{R}^{dK+1}$. Let $\boldsymbol{\beta} \in \mathbb{R}^{dK+1}$ denote the augmented parameter vector collecting the intercept and all basis coefficients, i.e., $\boldsymbol{\beta} = (\beta_0, \{\beta_{jk}\}_{j \in [d], k \in [K]})$. Under this formulation, the additive predictor becomes linear in the transformed feature space:

$$\beta_0 + \sum_{j=1}^d \sum_{k=1}^K \beta_{jk} \psi_k(x_j) = \langle \boldsymbol{\beta}, \tilde{\Phi}(\mathbf{x}) \rangle,$$

and hence the basis-expanded GAM reduces to a GLM problem in \mathbb{R}^{dK+1} .

The choice of basis functions impacts the theoretical properties of the estimator. We require the basis functions to be orthogonal (or at least linearly independent) with respect to the data distribution. If the basis functions are collinear, the covariance matrix of the augmented features $\mathbb{E}[\tilde{\Phi}(\mathbf{x})\tilde{\Phi}(\mathbf{x})^\top]$ becomes singular. This constitutes a degenerate case where the strong Minty condition (Assumption 4.1(iv)) fails (i.e., the modulus $\mu \rightarrow 0$), thereby compromising the uniqueness and stability guarantees of the VI estimator.

VI estimator for GAM. Following the framework established for GLMs, we define the VI estimator for GAMs by substituting the original covariates with the basis features. The empirical vector field $V_N : \mathbb{R}^{dK+1} \rightarrow \mathbb{R}^{dK+1}$ is

$$V_N(\boldsymbol{\beta}) := \mathbb{E}_{(\mathbf{x}, y) \sim \mathbb{P}_N} \left[\left(g^{-1}(\langle \boldsymbol{\beta}, \tilde{\Phi}(\mathbf{x}) \rangle) - y \right) \cdot \tilde{\Phi}(\mathbf{x}) \right].$$

The VI estimator $\hat{\boldsymbol{\beta}}_N$ is then defined as the solution to $V_N(\hat{\boldsymbol{\beta}}_N) = \mathbf{0}$ (whenever the solution is unique).

This formulation allows us to extend the theoretical guarantees of the VI estimator to the GAM setting. In particular, when the basis size K is fixed, the consistency and asymptotic normality results established for GLMs carry over by replacing the dimension factor $d + 1$ with $dK + 1$ and using the corresponding Lipschitz/Minty constants associated with the transformed features $\tilde{\Phi}(\mathbf{x})$.

Example. We examine the reconstruction of a GAM using the VI and MLE estimators in a toy experiment. Consider a GAM of the form

$$\mathbb{E}[y | \mathbf{x}] = g^{-1} \left(\sum_{j=1}^d f_j(x_j) \right), \quad \mathbf{x} \in [-1, 1]^d.$$

Each additive component f_j is expanded using a truncated Legendre basis without the constant term, which enforces identifiability via $f_j(0) = 0$, $f_j(\mathbf{x}) = \sum_{k=1}^K \beta_{jk} P_k(x_j)$, where P_k denotes the k -th Legendre polynomial on $[-1, 1]$. With this basis expansion, the GAM reduces to a finite-dimensional GLM, to which we apply both the VI and MLE updates.

Detailed experimental settings and results are deferred to Appendix G.2. Here we briefly summarize the main observations. For non-canonical links, VI typically exhibits more stable optimization behavior and slightly improved reconstruction of the underlying additive components. These results demonstrate that the VI estimator naturally extends to GAMs and retains its key advantages beyond linear predictors.

8 Discussion

This work clarifies the operator geometry underlying variational inequality formulations and shows that the behavior of the VI estimator is governed by the strong Minty modulus and the Lipschitz constant. These quantities determine convergence, stability, and statistical rates, suggesting a simple guideline for link-function design: larger Minty constants and smaller Lipschitz constants improve performance. Compared to MLE, which is constrained by the likelihood consistency of the composite loss $\ell \circ g^{-1}$, the VI framework offers greater flexibility in challenging regimes. In practice, VI is most effective when likelihood objectives exhibit flat or non-smooth regions, while canonical models remain well served by MLE. From a robustness perspective, the VI formulation decouples estimation from likelihood curvature, making stability depend on operator geometry rather than precise probabilistic specification.

Acknowledgment

This work is partially supported by an NSF DMS-2220495, CNS-2220387, NSF DMS-2134037, and the Coca-Cola Foundation.

References

- [1] Jean-Bernard Baillon and Georges Haddad. Quelques propriétés des opérateurs angle-bornés et n -cycloiquement monotones. *Israel Journal of Mathematics*, 26:137–150, 1977.
- [2] Yang Cao and Yao Xie. Poisson matrix recovery and completion. *IEEE Transactions on Signal Processing*, 64(6):1609–1620, 2015.
- [3] Xiuyuan Cheng, Tingnan Gong, and Yao Xie. Point processes with event time uncertainty. *arXiv preprint arXiv:2411.02694*, 2024.
- [4] Peter J. Green. Iteratively reweighted least squares for maximum likelihood estimation, and some robust and resistant alternatives. *Journal of the Royal Statistical Society: Series B*, 46(2):149–170, 1984.
- [5] Trevor Hastie and Robert Tibshirani. Generalized additive models. *Statistical science*, 1(3):297–310, 1986.
- [6] Niao He, Zaid Harchaoui, Yichen Wang, and Le Song. Point process estimation with mirror prox algorithms. *Applied Mathematics & Optimization*, 82(3):919–947, 2020.
- [7] Kevin Huang and Shuzhong Zhang. Beyond monotone variational inequalities: Solution methods and iteration complexities. *arXiv preprint arXiv:2304.04153*, 2023.
- [8] Anatoli Juditsky and Arkadi Nemirovski. Signal recovery by stochastic optimization. *Automation and Remote Control*, 80(10):1878–1893, 2019.

- [9] Anatoli Juditsky, Arkadi Nemirovski, Liyan Xie, and Yao Xie. Convex parameter recovery for interacting marked processes. *IEEE Journal on Selected Areas in Information Theory*, 1(3):799–813, 2020.
- [10] Anatoli Juditsky, Arkadi Nemirovski, Yao Xie, and Chen Xu. Generalized generalized linear models: Convex estimation and online bounds. *arXiv preprint arXiv:2304.13793*, 2023.
- [11] Sham M. Kakade, Varun Kanade, Ohad Shamir, and Adam Kalai. Efficient learning of generalized linear and single index models with isotonic regression. *Advances in Neural Information Processing Systems*, 24, 2011.
- [12] Adam Tauman Kalai and Ravi Sastry. The isotron algorithm: High-dimensional isotonic regression. In *Proceedings of the 22nd Annual Conference on Learning Theory (COLT)*, page 9, 2009.
- [13] Hamed Karimi, Julie Nutini, and Mark Schmidt. Linear convergence of gradient and proximal-gradient methods under the Polyak-Lojasiewicz condition. In *Joint European Conference on Machine Learning and Knowledge Discovery in Databases*, pages 795–811. Springer, 2016.
- [14] Harold J. Kushner and G. George Yin. *Stochastic Approximation and Recursive Algorithms and Applications*, volume 35 of *Stochastic Modelling and Applied Probability*. Springer, New York, NY, 2nd edition, 2003.
- [15] Mengqi Lou, Kabir Aladin Verchand, Sara Fridovich-Keil, and Ashwin Pananjady. Accurate, provable, and fast nonlinear tomographic reconstruction: A variational inequality approach. *arXiv preprint arXiv:2503.19925*, 2025.
- [16] Peter McCullagh and John A. Nelder. *Generalized Linear Models*. Chapman and Hall, London, 2nd edition, 1989.
- [17] John Ashworth Nelder and Robert W. M. Wedderburn. Generalized linear models. *Journal of the Royal Statistical Society Series A: Statistics in Society*, 135(3):370–384, 1972.
- [18] Yurii Nesterov. *Introductory Lectures on Convex Optimization: A Basic Course*, volume 87 of *Applied Optimization*. Springer, New York, NY, 2013.
- [19] R. Tyrrell Rockafellar and Roger J.-B. Wets. *Variational Analysis*, volume 317 of *Grundlehren der Mathematischen Wissenschaften*. Springer, Berlin, Heidelberg, 2nd edition, 2009.
- [20] Frank Rosenblatt. The perceptron: a probabilistic model for information storage and organization in the brain. *Psychological Review*, 65(6):386, 1958.
- [21] Aad W. Van der Vaart and Jon A. Wellner. Weak convergence. In *Weak Convergence and Empirical Processes: With Applications to Statistics*, pages 16–28. Springer, New York, NY, 1996.
- [22] Roman Vershynin. *High-Dimensional Probability: An Introduction with Applications in Data Science*, volume 47 of *Cambridge Series in Statistical and Probabilistic Mathematics*. Cambridge University Press, Cambridge, UK, 2018.
- [23] Jonathan Y Zhou and Yao Xie. Nonlinear time-series embedding by monotone variational inequality. In *Proceedings of the 13th International Conference on Learning Representations (ICLR)*, 2025.

A Notation

The notation in the paper is standard. Let \mathbb{R}^d denote the d -dimensional Euclidean space equipped with the inner product $\langle \mathbf{u}, \mathbf{v} \rangle := \mathbf{u}^\top \mathbf{v}$ and the induced norm $\|\mathbf{u}\| := \sqrt{\langle \mathbf{u}, \mathbf{u} \rangle}$. We write $\|\cdot\|_\infty$ for the infinity norm. For a convex set $\mathcal{B} \subseteq \mathbb{R}^d$, the Euclidean projection of a point $\boldsymbol{\beta}$ onto \mathcal{B} is defined as $\text{proj}_{\mathcal{B}}(\boldsymbol{\beta}) := \text{argmin}_{\boldsymbol{\beta}' \in \mathcal{B}} \|\boldsymbol{\beta}' - \boldsymbol{\beta}\|$, and the corresponding distance is given by $\text{dist}(\boldsymbol{\beta}, \mathcal{B}) := \|\boldsymbol{\beta} - \text{proj}_{\mathcal{B}}(\boldsymbol{\beta})\|$. For a general vector field $F : \mathbb{R}^d \rightarrow \mathbb{R}^d$, its solution set is defined as

$$\text{Sol}(F) := \left\{ \hat{\boldsymbol{\beta}} \in \mathbb{R}^d : \langle F(\hat{\boldsymbol{\beta}}), \boldsymbol{\beta} - \hat{\boldsymbol{\beta}} \rangle \geq 0, \forall \boldsymbol{\beta} \in \mathbb{R}^d \right\} = \left\{ \hat{\boldsymbol{\beta}} \in \mathbb{R}^d : F(\hat{\boldsymbol{\beta}}) = \mathbf{0} \right\}.$$

We use $\nabla F(\boldsymbol{\beta})$ to denote the Jacobian of F at $\boldsymbol{\beta}$. All random quantities are defined on a common probability space $(\Omega, \mathcal{F}, \mathbb{P})$. We consider i.i.d. samples $\{(\mathbf{x}^i, y^i)\}_{i=1}^N$ drawn from an unknown distribution \mathbb{P} , where each covariate $\mathbf{x}^i \in \mathbb{R}^d$ and response $y^i \in \mathbb{R}$. The empirical measure is denoted by $\mathbb{P}_N := \frac{1}{N} \sum_{i=1}^N \delta_{(\mathbf{x}^i, y^i)}$. Denote by $V_{(\mathbf{x}^i, y^i)}$ the per-sample VI operator and by $\mathcal{L}_{(\mathbf{x}^i, y^i)}$ the per-sample MLE negative log-likelihood function. We use \xrightarrow{d} to denote convergence in distribution. The notations $\mathcal{O}(\cdot)$ and $\tilde{\mathcal{O}}(\cdot)$ represent standard and logarithmically-tight asymptotic order, respectively, where $\tilde{\mathcal{O}}(f(N)) = \mathcal{O}(f(N) \text{polylog}(N))$. The notation $\mathcal{O}_p(\cdot)$ denotes stochastic order in probability, that is, $X_N = \mathcal{O}_p(a_N)$ means that the sequence $\{X_N/a_N\}$ is bounded in probability. Likewise, the notations $o(\cdot)$ and $o_p(\cdot)$ denote deterministic and stochastic convergence to zero, respectively.

B Detailed MLE and VI Optimization Landscape Derivations

In this appendix, we supplement the motivation provided in Section 3 with detailed mathematical derivations and a rigorous analysis of the optimization landscapes. First, we explicitly derive the gradients for several classical GLMs, including logistic, linear, exponential, and Poisson regression, to demonstrate the precise equivalence between MLE and VI formulation under canonical link functions (Appendix B.1). Second, we investigate the pathological behaviors of MLE in non-canonical settings. We provide an analytical calculation of the Hessian for the softplus link to quantify the ill-conditioning (flatness) of the MLE objective, and we present a detailed characterization of the non-convexity and non-smoothness induced by robust clipped links. These analyses highlight the structural advantages of the VI operator, which retains monotonicity even when the corresponding likelihood objective fails to be convex.

B.1 Examples of Vector Fields for Canonical MLE and VI

This section provides several representative examples of empirical vector fields arising from the MLE and the corresponding VI formulations. For each GLM, we derive the gradient of the empirical NLL function $\mathcal{L}_N(\boldsymbol{\beta})$ and verify that it coincides with the VI operator $V_N(\boldsymbol{\beta})$ under the canonical link function.

B.1.1 Logistic regression

For the binary logistic regression, the empirical NLL is given by

$$\mathcal{L}_N(\boldsymbol{\beta}) = -\frac{1}{N} \sum_{i=1}^N \left(y^i \log g^{-1}(\boldsymbol{\beta}^\top \tilde{\mathbf{x}}^i) + (1 - y^i) \log(1 - g^{-1}(\boldsymbol{\beta}^\top \tilde{\mathbf{x}}^i)) \right).$$

with gradient given by

$$\nabla \mathcal{L}_N(\boldsymbol{\beta}) = \frac{1}{N} \sum_{i=1}^N \frac{(g^{-1})'(\boldsymbol{\beta}^\top \tilde{\mathbf{x}}^i)}{g^{-1}(\boldsymbol{\beta}^\top \tilde{\mathbf{x}}^i)(1 - g^{-1}(\boldsymbol{\beta}^\top \tilde{\mathbf{x}}^i))} \cdot (g^{-1}(\boldsymbol{\beta}^\top \tilde{\mathbf{x}}^i) - y^i) \tilde{\mathbf{x}}^i.$$

For the logistic (sigmoid) link function $g^{-1}(z) = 1/(1 + e^{-z})$, one can show that $(g^{-1})'(z) = g^{-1}(z)(1 - g^{-1}(z))$, which simplifies the gradient to

$$\nabla \mathcal{L}_N(\boldsymbol{\beta}) = \frac{1}{N} \sum_{i=1}^N (g^{-1}(\boldsymbol{\beta}^\top \tilde{\mathbf{x}}^i) - y^i) \tilde{\mathbf{x}}^i,$$

and the last term above is identical to $V_N(\boldsymbol{\beta})$ in this case.

B.1.2 Linear regression

For the Gaussian (linear) model with an identity link, the empirical NLL is

$$\mathcal{L}_N(\boldsymbol{\beta}) = \frac{1}{N} \sum_{i=1}^N (g^{-1}(\boldsymbol{\beta}^\top \tilde{\mathbf{x}}^i) - y^i)^2,$$

whose gradient is

$$\nabla \mathcal{L}_N(\boldsymbol{\beta}) = \frac{1}{N} \sum_{i=1}^N (g^{-1})'(\boldsymbol{\beta}^\top \tilde{\mathbf{x}}^i) (g^{-1}(\boldsymbol{\beta}^\top \tilde{\mathbf{x}}^i) - y^i) \tilde{\mathbf{x}}^i.$$

With the identity link $g^{-1}(z) = z$, we have $(g^{-1})'(z) = 1$, leading to

$$\nabla \mathcal{L}_N(\boldsymbol{\beta}) = \frac{1}{N} \sum_{i=1}^N (g^{-1}(\boldsymbol{\beta}^\top \tilde{\mathbf{x}}^i) - y^i) \tilde{\mathbf{x}}^i = V_N(\boldsymbol{\beta}).$$

B.1.3 Exponential regression

For the exponential model, the empirical NLL with $\boldsymbol{\beta}^\top \tilde{\mathbf{x}}^i > 0$ is

$$\mathcal{L}_N(\boldsymbol{\beta}) = \frac{1}{N} \sum_{i=1}^N \left(\log g^{-1}(\boldsymbol{\beta}^\top \tilde{\mathbf{x}}^i) + y^i / g^{-1}(\boldsymbol{\beta}^\top \tilde{\mathbf{x}}^i) \right),$$

and the corresponding gradient is

$$\nabla \mathcal{L}_N(\boldsymbol{\beta}) = \frac{1}{N} \sum_{i=1}^N (g^{-1})'(\boldsymbol{\beta}^\top \tilde{\mathbf{x}}^i) \left(\frac{1}{g^{-1}(\boldsymbol{\beta}^\top \tilde{\mathbf{x}}^i)} - \frac{y^i}{g^{-1}(\boldsymbol{\beta}^\top \tilde{\mathbf{x}}^i)^2} \right) \tilde{\mathbf{x}}^i.$$

For the inverse link $g^{-1}(z) = z^{-1}$, we have $(g^{-1})'(z) = -z^{-2}$, yielding

$$\nabla \mathcal{L}_N(\boldsymbol{\beta}) = -\frac{1}{N} \sum_{i=1}^N (g^{-1}(\boldsymbol{\beta}^\top \tilde{\mathbf{x}}^i) - y^i) \tilde{\mathbf{x}}^i = -V_N(\boldsymbol{\beta}).$$

The gradient $\nabla \mathcal{L}_N(\boldsymbol{\beta})$ differs from $V_N(\boldsymbol{\beta})$ only by a sign, so minimizing the NLL is equivalent to solving $V_N(\boldsymbol{\beta}) = \mathbf{0}$, yielding the same optimal solution.

B.1.4 Poisson regression

For the Poisson model, the empirical NLL is

$$\mathcal{L}_N(\boldsymbol{\beta}) = \frac{1}{N} \sum_{i=1}^N \left(-y^i \log g^{-1}(\boldsymbol{\beta}^\top \tilde{\mathbf{x}}^i) + g^{-1}(\boldsymbol{\beta}^\top \tilde{\mathbf{x}}^i) \right).$$

The gradient is

$$\nabla \mathcal{L}_N(\boldsymbol{\beta}) = \frac{1}{N} \sum_{i=1}^N (g^{-1})'(\boldsymbol{\beta}^\top \tilde{\mathbf{x}}^i) \left(-\frac{y^i}{g^{-1}(\boldsymbol{\beta}^\top \tilde{\mathbf{x}}^i)} + 1 \right) \tilde{\mathbf{x}}^i.$$

With the exponential link $g^{-1}(z) = e^z$, we have $(g^{-1})'(z) = g^{-1}(z)$, so

$$\nabla \mathcal{L}_N(\boldsymbol{\beta}) = \frac{1}{N} \sum_{i=1}^N \left(g^{-1}(\boldsymbol{\beta}^\top \tilde{\mathbf{x}}^i) - y^i \right) \tilde{\mathbf{x}}^i = V_N(\boldsymbol{\beta}).$$

B.2 Flatness of MLE optimization landscape

We show that even when standard smooth link functions are applied to improve curvature, the resulting optimization landscape of the MLE can still exhibit considerably slower convergence than the VI formulation. This phenomenon is illustrated using the softplus link function, under which the MLE score and the VI operator define different estimating equations.

Recall the softplus inverse link function:

$$g^{-1}(z) = \log(1 + e^z), \quad (g^{-1})'(z) = \sigma(z) := \frac{1}{1 + e^{-z}},$$

and

$$(g^{-1})''(z) = \sigma(z)(1 - \sigma(z)).$$

For a single sample (\mathbf{x}, y) , the Poisson negative log-likelihood is

$$\mathcal{L}_{(\mathbf{x}, y)}(\boldsymbol{\beta}) = -y \log(g^{-1}(z)) + g^{-1}(z), \quad z = \tilde{\mathbf{x}}^\top \boldsymbol{\beta},$$

with gradient and Hessian given by, respectively,

$$\begin{aligned} \nabla \mathcal{L}_{(\mathbf{x}, y)}(\boldsymbol{\beta}) &= \sigma(z) \left(1 - \frac{y}{\log(1 + e^z)} \right) \tilde{\mathbf{x}}, \\ \nabla^2 \mathcal{L}_{(\mathbf{x}, y)}(\boldsymbol{\beta}) &= \left\{ \sigma(z)(1 - \sigma(z)) \left(1 - \frac{y}{\log(1 + e^z)} \right) + \frac{y \sigma(z)^2}{\log(1 + e^z)^2} \right\} \tilde{\mathbf{x}} \tilde{\mathbf{x}}^\top. \end{aligned}$$

On the other hand, the VI estimating operator is $V_{(\mathbf{x}, y)}(\boldsymbol{\beta}) = (g^{-1}(z) - y) \tilde{\mathbf{x}}$. At the population level, it follows that

$$\nabla V(\boldsymbol{\beta}) = \mathbb{E}_{\mathbf{x} \sim \mathbb{P}_{\mathbf{x}}} \left[\sigma(z) \cdot \tilde{\mathbf{x}} \tilde{\mathbf{x}}^\top \right], \quad \nabla^2 \mathcal{L}(\boldsymbol{\beta}) = \mathbb{E}_{\mathbf{x} \sim \mathbb{P}_{\mathbf{x}}} \left[\frac{\sigma(z)^2}{g^{-1}(z)} \cdot \tilde{\mathbf{x}} \tilde{\mathbf{x}}^\top \right].$$

Since $g^{-1}(z) \geq \sigma(z)$ for all z (with equality only as $z \rightarrow -\infty$), we have $\sigma(z) \geq \sigma(z)^2/g^{-1}(z)$ pointwise and hence

$$\nabla V(\boldsymbol{\beta}) - \nabla^2 \mathcal{L}(\boldsymbol{\beta}) = \mathbb{E}_{\mathbf{x} \sim \mathbb{P}_{\mathbf{x}}} \left[\left(\sigma(z) - \frac{\sigma(z)^2}{g^{-1}(z)} \right) \cdot \tilde{\mathbf{x}} \tilde{\mathbf{x}}^\top \right] \succeq \mathbf{0}.$$

Moreover, we know that

$$\frac{\sigma(z)}{\sigma^2(z)/g^{-1}(z)} = \frac{g^{-1}(z)}{\sigma(z)} = \frac{\log(1+e^z)(1+e^z)}{e^z} \rightarrow +\infty \quad \text{as } z \rightarrow +\infty,$$

which reveals a flat-growth regime in the right tail when the features are not linearly dependent (i.e., $\mathbb{E}_{\mathbf{x} \sim \mathbb{P}_{\mathbf{x}}}[\tilde{\mathbf{x}}\tilde{\mathbf{x}}^\top] \succ \mathbf{0}$): the curvature weight of the MLE decays relative to that of the VI formulation. Consequently, optimization solvers exhibit weaker local contraction when applied to the MLE, and statistical concentration bounds that depend on the curvature modulus become looser.

C Characterization of Minty Conditions

To start with, we introduce the following definition, which is widely used for solving variational inequalities, e.g., [7].

Definition C.1 (Strong Minty condition). *The vector field $F : \mathbb{R}^d \rightarrow \mathbb{R}^d$ satisfies the strong Minty condition with constant $\mu \geq 0$ if $\text{Sol}(F) \neq \emptyset$ and*

$$\langle F(\boldsymbol{\beta}), \boldsymbol{\beta} - \text{proj}_{\text{Sol}(F)}(\boldsymbol{\beta}) \rangle \geq \mu \cdot \text{dist}^2(\boldsymbol{\beta}, \text{Sol}(F)), \quad \forall \boldsymbol{\beta} \in \mathbb{R}^d.$$

The strong Minty condition plays a central role in the VI estimator. In this section, we first establish sufficient conditions under which this property holds and illustrate them through representative examples. We then discuss guiding principles for designing link functions that naturally satisfy or approximate the strong Minty condition in practice.

Definition C.2. *Given constants $\rho, \mu_{\text{EB}} > 0$, we introduce the following properties:*

- *F is said to be ρ -weakly monotone if*

$$\langle F(\boldsymbol{\beta}_2) - F(\boldsymbol{\beta}_1), \boldsymbol{\beta}_2 - \boldsymbol{\beta}_1 \rangle \geq -\frac{\rho}{2} \|\boldsymbol{\beta}_2 - \boldsymbol{\beta}_1\|^2, \quad \forall \boldsymbol{\beta}_1, \boldsymbol{\beta}_2 \in \mathbb{R}^d.$$

- *F is said to satisfy the error bound property with constant $\mu_{\text{EB}} > 0$ if*

$$\|F(\boldsymbol{\beta}) - F(\text{proj}_{\text{Sol}(F)}(\boldsymbol{\beta}))\| \geq \mu_{\text{EB}} \cdot \text{dist}(\boldsymbol{\beta}, \text{Sol}(F)), \quad \forall \boldsymbol{\beta} \in \mathbb{R}^d.$$

Weak monotonicity is a mild regularity condition that allows certain non-monotone vector fields while still ensuring local stability of the VI solution. In contrast, the error bound condition provides a geometric separation property: it quantifies how far a point $\boldsymbol{\beta}$ is from the solution set in terms of the magnitude of the operator, implying that the vector field $F(\boldsymbol{\beta})$ is uniformly separated from zero along the direction of its projection onto the solution set. Intuitively, this means that F grows at least linearly with the distance to the solution, forming a local conic region around the zero point. With these two conditions, we have the following implication.

Proposition C.3. *Suppose that the vector field $F : \mathbb{R}^d \rightarrow \mathbb{R}^d$ satisfies L -Lipschitz condition, i.e.,*

$$\|F(\boldsymbol{\beta}_2) - F(\boldsymbol{\beta}_1)\| \leq L \|\boldsymbol{\beta}_2 - \boldsymbol{\beta}_1\|.$$

Additionally, we assume that F satisfies the ρ -weakly monotone condition and the error bound property holds with μ_{EB} . If $\rho L < \mu_{\text{EB}}^2$, then the strong Minty condition holds with $\mu = \frac{\mu_{\text{EB}}^2 - \rho L}{L - \rho}$.

Proof. Since F satisfies the ρ -weakly monotone and L -Lipschitz condition, we know that $F(\boldsymbol{\beta}) + \rho\boldsymbol{\beta}$ is monotone and $L + \rho$ Lipschitz, then by Baillon-Haddad Lemma [1, Corollaire 10] we know that

$$\begin{aligned} & \langle F(\boldsymbol{\beta}) - F(\text{proj}_{\text{Sol}(F)}(\boldsymbol{\beta})) + \rho(\boldsymbol{\beta} - \text{proj}_{\text{Sol}(F)}(\boldsymbol{\beta})), \boldsymbol{\beta} - \text{proj}_{\text{Sol}(F)}(\boldsymbol{\beta}) \rangle \\ & \geq \frac{1}{L + \rho} \|F(\boldsymbol{\beta}) - F(\text{proj}_{\text{Sol}(F)}(\boldsymbol{\beta})) + \rho(\boldsymbol{\beta} - \text{proj}_{\text{Sol}(F)}(\boldsymbol{\beta}))\|^2 \end{aligned}$$

which implies that

$$\begin{aligned} & \frac{L - \rho}{L + \rho} \langle F(\boldsymbol{\beta}) - F(\text{proj}_{\text{Sol}(F)}(\boldsymbol{\beta})), \boldsymbol{\beta} - \text{proj}_{\text{Sol}(F)}(\boldsymbol{\beta}) \rangle \\ & \geq \frac{1}{L + \rho} \|F(\boldsymbol{\beta}) - F(\text{proj}_{\text{Sol}(F)}(\boldsymbol{\beta}))\|^2 - \frac{\rho L}{L + \rho} \|\boldsymbol{\beta} - \text{proj}_{\text{Sol}(F)}(\boldsymbol{\beta})\|^2. \end{aligned}$$

Combining this with the error bound property, we know that

$$\begin{aligned} & \langle F(\boldsymbol{\beta}) - F(\text{proj}_{\text{Sol}(F)}(\boldsymbol{\beta})), \boldsymbol{\beta} - \text{proj}_{\text{Sol}(F)}(\boldsymbol{\beta}) \rangle \\ & \geq \frac{\mu_{\text{EB}}^2}{L - \rho} \|\boldsymbol{\beta} - \text{proj}_{\text{Sol}(F)}(\boldsymbol{\beta})\|^2 - \frac{\rho L}{L - \rho} \|\boldsymbol{\beta} - \text{proj}_{\text{Sol}(F)}(\boldsymbol{\beta})\|^2 \\ & = \frac{\mu_{\text{EB}}^2 - \rho L}{L - \rho} \|\boldsymbol{\beta} - \text{proj}_{\text{Sol}(F)}(\boldsymbol{\beta})\|^2. \end{aligned}$$

The proof is complete. \square

It is straightforward to verify that if F is strongly monotone, then it implies the error bound property, which characterizes the local growth behavior around the solution set and implies the strong Minty condition. Moreover, we provide an example showing that F need not be monotone for the strong Minty condition to hold.

Example. In many practical systems, such as those encountered in signal processing and communications, the ideal input-output response is approximately linear. However, due to hardware imperfections or nonlinear circuit effects, small nonlinear distortions may arise. A simple model capturing such behavior is given by

$$g^{-1}(z) = z + 2 \sin(z) \cos(z).$$

The derivative of this function is

$$(g^{-1})'(z) = 1 + 2(\cos^2(z) - \sin^2(z)) = 3 \cos^2(z) - \sin^2(z),$$

which is not always positive; hence, g^{-1} is not a monotone function. Nevertheless, let $z^* = 0$ denote the solution to $g^{-1}(z) = 0$. Then

$$\langle g^{-1}(z) - g^{-1}(z^*), z - z^* \rangle = g^{-1}(z)z \geq z^2 + 2z \sin(z) \cos(z) = z(z + \sin(2z)) \geq \frac{1}{2}z^2.$$

This inequality confirms that, despite the lack of monotonicity, the mapping g^{-1} satisfies the strong Minty condition with modulus $\mu = 1/2$.

The following lemma shows that the vector field V_N satisfies the strong Minty condition when the inverse link function g^{-1} satisfies an averaged Minty's condition (which can be implied by the

strong monotonicity). With a fixed sample size N , we collect the covariates into the data matrix $\mathbf{X}_N \in \mathbb{R}^{N \times d}$ defined as

$$\mathbf{X}_N := \begin{bmatrix} x_1^1 & \cdots & x_d^1 \\ \vdots & \ddots & \vdots \\ x_1^N & \cdots & x_d^N \end{bmatrix},$$

where x_j^i denotes the j -th covariate of the i -th observation. A population version can be derived under analogous conditions.

Lemma C.4 (Sufficient Condition for Strong Minty Condition). *Suppose that the inverse link function g^{-1} satisfies the strong monotonicity with modulus $\mu_g \geq 0$ or the averaged strong Minty condition with $\text{Sol}(V_N) \neq \emptyset$ that*

$$\frac{1}{N} \sum_{i=1}^N \left(g^{-1}(\tilde{\mathbf{x}}^{i\top} \boldsymbol{\beta}) - y^i \right) \cdot \tilde{\mathbf{x}}^{i\top} (\boldsymbol{\beta} - \text{proj}_{\text{Sol}(V_N)}(\boldsymbol{\beta})) \geq \frac{\mu_g}{N} \cdot \sum_{i=1}^N \left| \tilde{\mathbf{x}}^{i\top} (\boldsymbol{\beta} - \text{proj}_{\text{Sol}(V_N)}(\boldsymbol{\beta})) \right|^2. \quad (\text{C.1})$$

Then the vector field V_N satisfies the strong Minty condition with modulus $\mu_g \sigma_N^2 / N$, where σ_N is the minimal singular value of $\tilde{\mathbf{X}}_N := [\mathbf{1} \ \mathbf{X}_N]$, i.e., for any $\boldsymbol{\beta} \in \mathbb{R}^{d+1}$

$$\langle V_N(\boldsymbol{\beta}), \boldsymbol{\beta} - \text{proj}_{\text{Sol}(V_N)}(\boldsymbol{\beta}) \rangle \geq \frac{\mu_g \sigma_N^2}{N} \cdot \|\boldsymbol{\beta} - \text{proj}_{\text{Sol}(V_N)}(\boldsymbol{\beta})\|^2.$$

Proof. Recall the definition that $V_N(\boldsymbol{\beta}) = \frac{1}{N} \sum_{i=1}^N (g^{-1}(\beta_0 + \sum_{j=1}^d \beta_j x_j^i) - y^i) \cdot \tilde{\mathbf{x}}^i$. This together with (C.1) implies that

$$\begin{aligned} \langle V_N(\boldsymbol{\beta}), \boldsymbol{\beta} - \text{proj}_{\text{Sol}(V_N)}(\boldsymbol{\beta}) \rangle &= \left\langle \frac{1}{N} \sum_{i=1}^N \left(g^{-1} \left(\beta_0 + \sum_{j=1}^d \beta_j x_j^i \right) - y^i \right) \cdot \tilde{\mathbf{x}}^i, \boldsymbol{\beta} - \text{proj}_{\text{Sol}(V_N)}(\boldsymbol{\beta}) \right\rangle \\ &\geq \frac{\mu_g}{N} \cdot \sum_{i=1}^N \left[\left| \tilde{\mathbf{x}}^{i\top} (\boldsymbol{\beta} - \text{proj}_{\text{Sol}(V_N)}(\boldsymbol{\beta})) \right|^2 \right] \\ &= \frac{\mu_g}{N} \cdot \left\| \tilde{\mathbf{X}}_N (\boldsymbol{\beta} - \text{proj}_{\text{Sol}(V_N)}(\boldsymbol{\beta})) \right\|^2 \\ &\geq \frac{\mu_g \sigma_N^2}{N} \cdot \|\boldsymbol{\beta} - \text{proj}_{\text{Sol}(V_N)}(\boldsymbol{\beta})\|^2. \end{aligned}$$

This establishes that the averaged strong Minty condition (C.1) indeed implies the desired inequality for V_N . It remains to show that (C.1) itself is guaranteed whenever the inverse link function g^{-1} is μ_g -strongly monotone. In this case, for any $\boldsymbol{\beta} \in \mathbb{R}^{d+1}$ we have

$$\begin{aligned} &\sum_{i=1}^N \left\langle g^{-1}(\tilde{\mathbf{x}}^{i\top} \boldsymbol{\beta}) - y^i, \tilde{\mathbf{x}}^{i\top} (\boldsymbol{\beta} - \text{proj}_{\text{Sol}(V_N)}(\boldsymbol{\beta})) \right\rangle \\ &= \sum_{i=1}^N \left\langle \left(g^{-1}(\tilde{\mathbf{x}}^{i\top} \boldsymbol{\beta}) - g^{-1}(\tilde{\mathbf{x}}^{i\top} \text{proj}_{\text{Sol}(V_N)}(\boldsymbol{\beta})) \right) \cdot \tilde{\mathbf{x}}^i, \boldsymbol{\beta} - \text{proj}_{\text{Sol}(V_N)}(\boldsymbol{\beta}) \right\rangle \\ &\geq \mu_g \sum_{i=1}^N \left| \tilde{\mathbf{x}}^{i\top} (\boldsymbol{\beta} - \text{proj}_{\text{Sol}(V_N)}(\boldsymbol{\beta})) \right|^2, \end{aligned}$$

where the equality is from the definition of $\text{proj}_{\text{Sol}(V_N)}(\boldsymbol{\beta})$, namely that it is a solution of

$$V_N(\text{proj}_{\text{Sol}(V_N)}(\boldsymbol{\beta})) = \frac{1}{N} \sum_{i=1}^N (g^{-1}(\tilde{\boldsymbol{x}}^{i\top} \text{proj}_{\text{Sol}(V_N)}(\boldsymbol{\beta})) - y^i) \cdot \tilde{\boldsymbol{x}}^i = \mathbf{0}.$$

Then (C.1) holds. The proof is complete. \square

D Proofs for Section 4

Lemma D.1. *Suppose that Assumptions 4.1 (i)-(iii) hold. Then for every (\boldsymbol{x}, y) we have*

$$\|V_{(\boldsymbol{x}, y)}(\boldsymbol{\beta})\|_\infty \leq RM, \quad \|V_{(\boldsymbol{x}, y)}(\boldsymbol{\beta})\| \leq \sqrt{d+1}RM,$$

and

$$\|V_{(\boldsymbol{x}, y)}(\boldsymbol{\beta}_2) - V_{(\boldsymbol{x}, y)}(\boldsymbol{\beta}_1)\| \leq (LdM^2 + L) \cdot \|\boldsymbol{\beta}_2 - \boldsymbol{\beta}_1\|.$$

Proof. First, from Assumptions 4.1 (ii)-(iii) it follows that $\|\boldsymbol{x}\|_\infty \leq M$, $\|\boldsymbol{x}\| \leq \sqrt{d}M$ and

$$\left| g^{-1} \left(\beta_0 + \sum_{j=1}^d \beta_j x_j \right) - y \right| \leq R.$$

Then we have the upper bound (assuming $M \geq 1$) that

$$\begin{aligned} \|V_{(\boldsymbol{x}, y)}(\boldsymbol{\beta})\|_\infty &\leq \left| g^{-1} \left(\beta_0 + \sum_{j=1}^d \beta_j x_j \right) - y \right| \cdot \|\tilde{\boldsymbol{x}}\|_\infty \leq RM, \\ \|V_{(\boldsymbol{x}, y)}(\boldsymbol{\beta})\| &\leq \left| g^{-1} \left(\beta_0 + \sum_{j=1}^d \beta_j x_j \right) - y \right| \cdot \|\tilde{\boldsymbol{x}}\| \leq \sqrt{d+1}RM. \end{aligned}$$

Next, for the Lipschitz constant of $V_{(\boldsymbol{x}, y)}$, one has that

$$\begin{aligned} \|V_{(\boldsymbol{x}, y)}(\boldsymbol{\beta}') - V_{(\boldsymbol{x}, y)}(\boldsymbol{\beta})\| &= \left\| \left(g^{-1} \left(\beta'_0 + \sum_{j=1}^d \beta'_j x_j \right) - g^{-1} \left(\beta_0 + \sum_{j=1}^d \beta_j x_j \right) \right) \cdot \tilde{\boldsymbol{x}} \right\| \\ &\leq L \|\tilde{\boldsymbol{x}}\| \cdot \left| \beta'_0 - \beta_0 + \sum_{j=1}^d \beta'_j x_j - \sum_{j=1}^d \beta_j x_j \right| \\ &\leq L \|\tilde{\boldsymbol{x}}\|^2 \|\boldsymbol{\beta}' - \boldsymbol{\beta}\| \\ &\leq (LdM^2 + L) \cdot \|\boldsymbol{\beta}' - \boldsymbol{\beta}\|. \end{aligned}$$

The proof is complete. \square

Proof of Theorem 4.1

Proof. First, from the strong Minty condition in Assumption 4.1 (iv), we know that

$$\mu \|\boldsymbol{\beta}^* - \hat{\boldsymbol{\beta}}_N\|^2 \leq \langle V_N(\boldsymbol{\beta}^*), \boldsymbol{\beta}^* - \hat{\boldsymbol{\beta}}_N \rangle \leq \|V_N(\boldsymbol{\beta}^*)\| \|\boldsymbol{\beta}^* - \hat{\boldsymbol{\beta}}_N\|,$$

which implies

$$\mu \|\boldsymbol{\beta}^* - \hat{\boldsymbol{\beta}}_N\| \leq \|V_N(\boldsymbol{\beta}^*)\|. \quad (\text{D.1})$$

Recall the definition that for any $\boldsymbol{\beta} \in \mathbb{R}^{d+1}$

$$V_N(\boldsymbol{\beta}) = \mathbb{E}_{(\mathbf{x}, y) \sim \mathbb{P}_N} \left[\left(g^{-1} \left(\beta_0 + \sum_{j=1}^d \beta_j x_j \right) - y \right) \cdot \tilde{\mathbf{x}} \right] = \mathbb{E}_{(\mathbf{x}, y) \sim \mathbb{P}_N} V_{(\mathbf{x}, y)}(\boldsymbol{\beta}).$$

Then we know from Lemma D.1 that

$$\|V_N(\boldsymbol{\beta}^*)\|_\infty \leq RM.$$

As $V(\boldsymbol{\beta}^*) = \mathbf{0}$, by applying the Hoeffding's inequality [22, Theorem 2.2.6], it follows that for any $t > 0$ and $j \in \{0, \dots, d\}$,

$$\begin{aligned} \mathbb{P}(|V_N(\boldsymbol{\beta}^*)_j| \geq t) &= \mathbb{P}(|V_N(\boldsymbol{\beta}^*)_j - V(\boldsymbol{\beta}^*)_j| \geq t) \\ &= \mathbb{P}(V_N(\boldsymbol{\beta}^*)_j - V(\boldsymbol{\beta}^*)_j \geq t) + \mathbb{P}(-V_N(\boldsymbol{\beta}^*)_j + V(\boldsymbol{\beta}^*)_j \geq t) \\ &\leq 2 \exp\left(-\frac{Nt^2}{2R^2M^2}\right). \end{aligned}$$

Using the union bound (i.e., Boole's inequality),

$$\begin{aligned} \mathbb{P}(\|V_N(\boldsymbol{\beta}^*)\| \geq t) &\leq \mathbb{P}\left(\sqrt{d+1}\|V_N(\boldsymbol{\beta}^*)\|_\infty \geq t\right) \\ &\leq \sum_{j=0}^d \mathbb{P}\left(|V_N(\boldsymbol{\beta}^*)_j| \geq \frac{t}{\sqrt{d+1}}\right) \leq 2(d+1) \exp\left(-\frac{Nt^2}{2(d+1)R^2M^2}\right). \end{aligned}$$

Equivalently, for any $\epsilon \in (0, 1)$, set $t = RM\sqrt{2(d+1)\ln(2(d+1)/\epsilon)/N}$. Then with probability at least $1 - \epsilon$,

$$\|V_N(\boldsymbol{\beta}^*)\| \leq RM\sqrt{\frac{2(d+1)\ln(2(d+1)/\epsilon)}{N}}.$$

Combining this with (D.1), we derive the desired results. \square

Proof of Lemma 4.2

Proof. Let $u := \langle \tilde{\mathbf{x}}, \boldsymbol{\beta}^* \rangle$ and $\delta_t := \langle \tilde{\mathbf{x}}, \mathbf{h}_t \rangle$ for some sequence $\mathbf{h}_t \rightarrow \mathbf{h}$ as $t \downarrow 0$. Then

$$\frac{V(\boldsymbol{\beta}^* + t\mathbf{h}_t) - V(\boldsymbol{\beta}^*)}{t} = \mathbb{E}_{(\mathbf{x}, y) \sim \mathbb{P}} \left[\frac{g^{-1}(u + t\delta_t) - g^{-1}(u)}{t} \tilde{\mathbf{x}} \right]. \quad (\text{D.2})$$

Since $\mathbb{P}(u \in \mathcal{K}) = 0$ by Assumption 4.2, g^{-1} is differentiable at u almost surely, and therefore

$$g^{-1}(u + t\delta_t) = g^{-1}(u) + (g^{-1})'(u) t\delta_t + o(t|\delta_t|) \quad \text{a.s.}$$

Hence, pointwise almost surely,

$$\frac{g^{-1}(u + t\delta_t) - g^{-1}(u)}{t} \tilde{\mathbf{x}} \rightarrow (g^{-1})'(u) \langle \tilde{\mathbf{x}}, \mathbf{h} \rangle \tilde{\mathbf{x}}. \quad (\text{D.3})$$

Moreover, by the global Lipschitz property of g^{-1} with constant L ,

$$\left\| \frac{g^{-1}(u + t\delta_t) - g^{-1}(u)}{t} \tilde{\mathbf{x}} \right\| \leq L |\delta_t| \|\tilde{\mathbf{x}}\| \leq L \|\tilde{\mathbf{x}}\|^2 \|\mathbf{h}_t\|.$$

Under Assumption 4.1, we have $\|\tilde{\mathbf{x}}\|^2 \leq 1 + dM^2$, so the right-hand side is bounded by $L(1 + dM^2)\|\mathbf{h}_t\|$, which is integrable and independent of t since $\|\mathbf{h}_t\|$ is bounded. From (D.2) and (D.3) with the dominated convergence theorem, it follows that

$$\frac{V(\boldsymbol{\beta}^* + t\mathbf{h}_t) - V(\boldsymbol{\beta}^*)}{t} \rightarrow \mathbb{E}_{(\mathbf{x},y) \sim \mathbb{P}} \left[(g^{-1})'(\langle \tilde{\mathbf{x}}, \boldsymbol{\beta}^* \rangle) \tilde{\mathbf{x}} \tilde{\mathbf{x}}^\top \right] \mathbf{h}.$$

Thus V is Fréchet differentiable at $\boldsymbol{\beta}^*$ with gradient $\nabla V(\boldsymbol{\beta}^*)$ as claimed. \square

Proof of Theorem 4.3

Proof. By Assumption 4.1, $|g^{-1}(\langle \tilde{\mathbf{x}}, \boldsymbol{\beta}^* \rangle) - y| \leq R$, $\|\mathbf{x}\|^2 \leq dM^2$, and g^{-1} is Lipschitz. Hence,

$$\mathbb{E}_{(\mathbf{x},y) \sim \mathbb{P}} [\|V_{(\mathbf{x},y)}(\boldsymbol{\beta}^*)\|^2] \leq \mathbb{E}_{(\mathbf{x},y) \sim \mathbb{P}} [|g^{-1}(\langle \tilde{\mathbf{x}}, \boldsymbol{\beta}^* \rangle) - y|^2 \|\tilde{\mathbf{x}}\|^2] \leq R^2(1 + dM^2) < \infty.$$

Therefore, when $(\mathbf{x}^i, y^i)_{i=1}^N$ are i.i.d. samples, the random vectors $V_{(\mathbf{x}^i, y^i)}(\boldsymbol{\beta}^*)$ are i.i.d. with mean zero and covariance matrix Γ (finite and positive definite by Assumption (A2)). Applying the multivariate central limit theorem yields

$$\sqrt{N}(V_N(\boldsymbol{\beta}^*) - V(\boldsymbol{\beta}^*)) \xrightarrow{d} \mathcal{N}(\mathbf{0}, \Gamma). \quad (\text{D.4})$$

Adding and subtracting $V(\hat{\boldsymbol{\beta}}_N)$ and $V(\boldsymbol{\beta}^*)$ on $V_N(\hat{\boldsymbol{\beta}}_N)$ yields

$$\mathbf{0} = V_N(\hat{\boldsymbol{\beta}}_N) = V_N(\boldsymbol{\beta}^*) + \underbrace{V(\hat{\boldsymbol{\beta}}_N) - V(\boldsymbol{\beta}^*)}_{\text{population increment}} + \underbrace{(V_N(\hat{\boldsymbol{\beta}}_N) - V(\hat{\boldsymbol{\beta}}_N)) - (V_N(\boldsymbol{\beta}^*) - V(\boldsymbol{\beta}^*))}_{=: R_N}. \quad (\text{D.5})$$

By the Fréchet differentiability of V at $\boldsymbol{\beta}^*$ (Lemma 4.2), we have the local linearization

$$V(\hat{\boldsymbol{\beta}}_N) - V(\boldsymbol{\beta}^*) = \nabla V(\boldsymbol{\beta}^*)(\hat{\boldsymbol{\beta}}_N - \boldsymbol{\beta}^*) + r_N, \quad \|r_N\| = o(\|\hat{\boldsymbol{\beta}}_N - \boldsymbol{\beta}^*\|). \quad (\text{D.6})$$

From Lemma D.1, the sample operator $V_{(\mathbf{x},y)}$ is $(LdM^2 + L)$ -Lipschitz. Therefore,

$$R_N = [\mathbb{E}_N - \mathbb{E}] \left(V_{(\cdot)}(\hat{\boldsymbol{\beta}}_N) - V_{(\cdot)}(\boldsymbol{\beta}^*) \right)$$

represents an empirical process evaluated on a Lipschitz-indexed function class. For $0 < r \leq 1$, define

$$\mathcal{F}_r := \left\{ f_{\boldsymbol{\beta}}(\cdot) := \frac{V_{(\cdot)}(\boldsymbol{\beta}) - V_{(\cdot)}(\boldsymbol{\beta}^*)}{\|\boldsymbol{\beta} - \boldsymbol{\beta}^*\|} : \|\boldsymbol{\beta} - \boldsymbol{\beta}^*\| \leq r \right\}.$$

Each function $f_{\boldsymbol{\beta}}$ is uniformly bounded by the envelope $LdM^2 + L$, and the class \mathcal{F}_r is a finite-dimensional (Euclidean) Lipschitz image of a ball in \mathbb{R}^{d+1} . Such finite-dimensional Lipschitz (parametric) classes have a covering numbers that grow polynomially in $1/\epsilon$, a direct consequence of the parameter space being a subset of \mathbb{R}^{d+1} (see [21, Theorem 2.7.11]). This polynomial entropy bound, together with the existence of a square-integrable envelope, implies that \mathcal{F}_r is \mathbb{P} -Donsker by [21, Theorem 2.5.2]. Consequently,

$$\sup_{f \in \mathcal{F}_r} \left\| \sqrt{N}[\mathbb{E}_N - \mathbb{E}]f \right\| = O_p(1). \quad (\text{D.7})$$

Since $\|\hat{\boldsymbol{\beta}}_N - \boldsymbol{\beta}^*\| = O_p(N^{-1/2})$ by Theorem 4.1, we have

$$\mathbb{P}(\|\hat{\boldsymbol{\beta}}_N - \boldsymbol{\beta}^*\| \leq r) \rightarrow 1.$$

Then on the event $\mathcal{A}_N := \{\|\hat{\boldsymbol{\beta}}_N - \boldsymbol{\beta}^*\| \leq r\}$ it follows

$$\begin{aligned} \sqrt{N} \|R_N\| &= \sqrt{N} \left\| [\mathbb{E}_N - \mathbb{E}] \left(V_{(\cdot)}(\hat{\boldsymbol{\beta}}_N) - V_{(\cdot)}(\boldsymbol{\beta}^*) \right) \right\| = \left\| \sqrt{N} [\mathbb{E}_N - \mathbb{E}] f_{\hat{\boldsymbol{\beta}}_N} \right\| \cdot \|\hat{\boldsymbol{\beta}}_N - \boldsymbol{\beta}^*\| \\ &\leq \sup_{f \in \mathcal{F}_r} \left\| \sqrt{N} [\mathbb{E}_N - \mathbb{E}] f \right\| \cdot \|\hat{\boldsymbol{\beta}}_N - \boldsymbol{\beta}^*\|. \end{aligned}$$

This together with $\|\hat{\boldsymbol{\beta}}_N - \boldsymbol{\beta}^*\| = O_p(N^{-1/2})$ and (D.7), we conclude on \mathcal{A}_N that

$$\sqrt{N} \|R_N\| = O_p(1) \cdot O_p(N^{-1/2}) = o_p(1).$$

Since $\mathbb{P}(\mathcal{A}_N^c) \rightarrow 0$, the same conclusion holds unconditionally:

$$\|R_N\| = o_p(N^{-1/2}).$$

Substitute (D.6) into (D.5):

$$\mathbf{0} = V_N(\boldsymbol{\beta}^*) + \nabla V(\boldsymbol{\beta}^*)(\hat{\boldsymbol{\beta}}_N - \boldsymbol{\beta}^*) + r_N + R_N.$$

Rearranging terms gives

$$\sqrt{N}(\hat{\boldsymbol{\beta}}_N - \boldsymbol{\beta}^*) = -\nabla V(\boldsymbol{\beta}^*)^{-1} \sqrt{N}(V_N(\boldsymbol{\beta}^*) - V(\boldsymbol{\beta}^*)) - \nabla V(\boldsymbol{\beta}^*)^{-1} \sqrt{N}(r_N + R_N).$$

The first term converges in distribution to $\mathcal{N}(0, \nabla V(\boldsymbol{\beta}^*)^{-1} \Gamma \nabla V(\boldsymbol{\beta}^*)^{-\top})$ by (D.4). On the other hand, $\sqrt{N} \|r_N\| = o_p(1)$ and $\sqrt{N} \|R_N\| = o_p(1)$, the second term vanishes in probability. Applying Slutsky's theorem gives

$$\sqrt{N}(\hat{\boldsymbol{\beta}}_N - \boldsymbol{\beta}^*) \xrightarrow{d} \mathcal{N}\left(\mathbf{0}, \nabla V(\boldsymbol{\beta}^*)^{-1} \Gamma \nabla V(\boldsymbol{\beta}^*)^{-\top}\right).$$

The proof is complete. \square

E Comparison of Asymptotic Efficiency between VI and MLE

A classical result in asymptotic statistics states that the MLE is asymptotically efficient, namely, it is consistent, asymptotically unbiased, and attains the Cramér–Rao lower bound (CRB) under correct model specification. The asymptotic covariance of the proposed VI estimator,

$$\Sigma_{\text{VI}} = \nabla V(\boldsymbol{\beta}^*)^{-1} \Gamma \nabla V(\boldsymbol{\beta}^*)^{-\top},$$

shares the same “sandwich” structure as that of the MLE,

$$\Sigma_{\text{MLE}} = (\nabla^2 \mathcal{L}(\boldsymbol{\beta}^*))^{-1} \text{Cov}(\nabla \mathcal{L}_{(x,y)}(\boldsymbol{\beta}^*)) (\nabla^2 \mathcal{L}(\boldsymbol{\beta}^*))^{-\top},$$

where the expected Hessian and the score covariance are given by

$$\nabla^2 \mathcal{L}(\boldsymbol{\beta}^*) = \mathbb{E}_{(x,y) \sim \mathbb{P}} \left[\frac{(g^{-1})'(\tilde{\mathbf{x}}^\top \boldsymbol{\beta}^*)^2}{\text{Var}(y | \tilde{\mathbf{x}})} \tilde{\mathbf{x}} \tilde{\mathbf{x}}^\top \right],$$

and

$$\begin{aligned} \text{Cov}(\nabla \mathcal{L}_{(x,y)}(\boldsymbol{\beta}^*)) &:= \mathbb{E}_{(x,y) \sim \mathbb{P}} \left[\nabla \mathcal{L}_{(x,y)}(\boldsymbol{\beta}^*) \nabla \mathcal{L}_{(x,y)}(\boldsymbol{\beta}^*)^\top \right] \\ &= \mathbb{E}_{(x,y) \sim \mathbb{P}} \left[\frac{(y - g^{-1}(\tilde{\mathbf{x}}^\top \boldsymbol{\beta}^*))^2 (g^{-1})'(\tilde{\mathbf{x}}^\top \boldsymbol{\beta}^*)^2}{\text{Var}(y | \tilde{\mathbf{x}})^2} \tilde{\mathbf{x}} \tilde{\mathbf{x}}^\top \right]. \end{aligned}$$

For correctly specified models, the information identity

$$\text{Cov}(\nabla \mathcal{L}_{(x,y)}(\boldsymbol{\beta}^*)) = \nabla^2 \mathcal{L}(\boldsymbol{\beta}^*) = I(\boldsymbol{\beta}^*)$$

holds, and the MLE achieves the Fisher information bound $I(\boldsymbol{\beta}^*)^{-1}$, attaining the CRB. In the following remark, we show that the MLE can indeed be asymptotically more efficient than the VI estimator under correct model specification. Their asymptotic covariances coincide only when the link function is canonical. This observation does not contradict our earlier discussion, as the VI estimator may still outperform the MLE in the presence of model or variance misspecification.

For correctly specified models with general link functions, the VI estimator generally does not satisfy the corresponding identity $\Gamma = \nabla V(\boldsymbol{\beta}^*)$, since the residual covariance and the Jacobian $\nabla V(\boldsymbol{\beta}^*)$ coincide only for special canonical links. Let

$$\Sigma_{\text{MLE}}^{-1} = \mathbb{E} \left[\frac{(g^{-1})'(\tilde{\mathbf{x}}^\top \boldsymbol{\beta}^*)^2}{\text{Var}(y | \tilde{\mathbf{x}})} \tilde{\mathbf{x}} \tilde{\mathbf{x}}^\top \right], \quad \mathbf{r}_1 = \sqrt{\text{Var}(y | \tilde{\mathbf{x}})} \tilde{\mathbf{x}}, \quad \mathbf{r}_2 = \frac{(g^{-1})'(\tilde{\mathbf{x}}^\top \boldsymbol{\beta}^*)}{\sqrt{\text{Var}(y | \tilde{\mathbf{x}})}} \tilde{\mathbf{x}}.$$

Then $\mathbb{E}[\mathbf{r}_1 \mathbf{r}_1^\top] = \Gamma$, $\mathbb{E}[\mathbf{r}_2 \mathbf{r}_2^\top] = \Sigma_{\text{MLE}}^{-1}$, $\mathbb{E}[\mathbf{r}_1 \mathbf{r}_2^\top] = \nabla V(\boldsymbol{\beta}^*)$, and hence the block moment matrix

$$\begin{bmatrix} \Gamma & \nabla V(\boldsymbol{\beta}^*) \\ \nabla V(\boldsymbol{\beta}^*) & \Sigma_{\text{MLE}}^{-1} \end{bmatrix} \succeq \mathbf{0}.$$

By the Schur complement, this implies the MLE is never less efficient than the VI estimator, i.e.,

$$\Sigma_{\text{MLE}} \preceq \Sigma_{\text{VI}}.$$

The equality holds if and only if \mathbf{r}_1 and \mathbf{r}_2 are a.s. linearly dependent, i.e., up to a constant $c > 0$,

$$\mathbb{E}[(y - g^{-1}(\tilde{\mathbf{x}}^\top \boldsymbol{\beta}^*))^2 | \tilde{\mathbf{x}}] = c \cdot (g^{-1})'(\tilde{\mathbf{x}}^\top \boldsymbol{\beta}^*) \quad \text{a.s. in } \tilde{\mathbf{x}},$$

which corresponds to the case where the link g is canonical (up to a constant scale). Hence, under correct specification, the MLE dominates the VI estimator in efficiency, with equality attained exactly for canonical links. As a result, the VI estimator may exhibit a loss of statistical efficiency relative to the MLE, for which the MLE is asymptotically optimal in the sense of attaining the CRB. Nevertheless, when the model or variance component is misspecified, the VI formulation, which relies solely on the mean relation, remains consistent and may even achieve a smaller asymptotic variance for the mean component, providing a robust alternative to likelihood-based estimation.

F Proofs for Section 5

Proof of Theorem 5.1

Proof. From the update rule of the fixed-point iterative method, the iterates satisfy

$$\boldsymbol{\beta}^{t+1} = \boldsymbol{\beta}^t - \eta V_N(\boldsymbol{\beta}^t), \quad \hat{\boldsymbol{\beta}}_N = \hat{\boldsymbol{\beta}}_N - \eta V_N(\hat{\boldsymbol{\beta}}_N),$$

where $\hat{\boldsymbol{\beta}}_N$ is a fixed point of the operator V_N , i.e., $V_N(\hat{\boldsymbol{\beta}}_N) = \mathbf{0}$. It then follows that

$$\|\boldsymbol{\beta}^{t+1} - \hat{\boldsymbol{\beta}}_N\|^2 = \|\boldsymbol{\beta}^t - \eta V_N(\boldsymbol{\beta}^t) - \hat{\boldsymbol{\beta}}_N + \eta V_N(\hat{\boldsymbol{\beta}}_N)\|^2.$$

Expanding the square gives

$$\|\boldsymbol{\beta}^{t+1} - \hat{\boldsymbol{\beta}}_N\|^2 = \|\boldsymbol{\beta}^t - \hat{\boldsymbol{\beta}}_N\|^2 - 2\eta \langle \boldsymbol{\beta}^t - \hat{\boldsymbol{\beta}}_N, V_N(\boldsymbol{\beta}^t) - V_N(\hat{\boldsymbol{\beta}}_N) \rangle + \eta^2 \|V_N(\boldsymbol{\beta}^t) - V_N(\hat{\boldsymbol{\beta}}_N)\|^2.$$

By the strong Minty monotonicity condition in Assumption 4.1 and the Lipschitz continuity in Lemma D.1, we have

$$\langle V_N(\boldsymbol{\beta}^t) - V_N(\hat{\boldsymbol{\beta}}_N), \boldsymbol{\beta}^t - \hat{\boldsymbol{\beta}}_N \rangle \geq \mu \|\boldsymbol{\beta}^t - \hat{\boldsymbol{\beta}}_N\|^2, \quad \|V_N(\boldsymbol{\beta}^t) - V_N(\hat{\boldsymbol{\beta}}_N)\| \leq (LdM^2 + L)\|\boldsymbol{\beta}^t - \hat{\boldsymbol{\beta}}_N\|.$$

Substituting these bounds gives

$$\|\boldsymbol{\beta}^{t+1} - \hat{\boldsymbol{\beta}}_N\|^2 \leq (1 - 2\eta\mu + \eta^2 L^2(1 + dM^2)^2) \|\boldsymbol{\beta}^t - \hat{\boldsymbol{\beta}}_N\|^2.$$

Choosing $\eta = \mu/(L^2(1 + dM^2)^2)$ yields

$$\|\boldsymbol{\beta}^{t+1} - \hat{\boldsymbol{\beta}}_N\|^2 \leq \left(1 - \frac{\mu^2}{L^2(1 + dM^2)^2}\right) \|\boldsymbol{\beta}^t - \hat{\boldsymbol{\beta}}_N\|^2.$$

By applying the above bound recursively, we obtain the claimed linear convergence rate of Algorithm 1. Combining this result with Theorem 4.1 further yields with the probability at least $1 - \epsilon$,

$$\begin{aligned} \|\boldsymbol{\beta}^t - \boldsymbol{\beta}^*\| &\leq \|\boldsymbol{\beta}^t - \hat{\boldsymbol{\beta}}_N\| + \|\hat{\boldsymbol{\beta}}_N - \boldsymbol{\beta}^*\| \\ &\leq \left(1 - \frac{\mu^2}{L^2(1 + dM^2)^2}\right)^{t/2} \|\boldsymbol{\beta}^0 - \hat{\boldsymbol{\beta}}_N\| + \frac{RM}{\mu} \sqrt{\frac{2(d+1)\ln(2(d+1)/\epsilon)}{N}}. \end{aligned}$$

The proof is complete. \square

Proof of Theorem 5.2

Proof. From the update rule we know that

$$\begin{aligned} \|\boldsymbol{\beta}^{t+1} - \boldsymbol{\beta}^*\|^2 &= \|\boldsymbol{\beta}^t - \eta^t V_{(\mathbf{x}^t, \mathbf{y}^t)}(\boldsymbol{\beta}^t) - \boldsymbol{\beta}^*\|^2 \\ &= \|\boldsymbol{\beta}^t - \boldsymbol{\beta}^*\|^2 - 2\eta^t \langle V_{(\mathbf{x}^t, \mathbf{y}^t)}(\boldsymbol{\beta}^t), \boldsymbol{\beta}^t - \boldsymbol{\beta}^* \rangle + (\eta^t)^2 \|V_{(\mathbf{x}^t, \mathbf{y}^t)}(\boldsymbol{\beta}^t)\|^2. \end{aligned}$$

Taking expectations and using the law of total expectation yields

$$\frac{1}{2} \mathbb{E} \|\boldsymbol{\beta}^{t+1} - \boldsymbol{\beta}^*\|^2 \leq \frac{1}{2} \mathbb{E} \|\boldsymbol{\beta}^t - \boldsymbol{\beta}^*\|^2 - \eta^t \mathbb{E} [\langle V_{(\mathbf{x}^t, \mathbf{y}^t)}(\boldsymbol{\beta}^t), \boldsymbol{\beta}^t - \boldsymbol{\beta}^* \rangle] + \frac{1}{2} (\eta^t)^2 \mathbb{E} \|V_{(\mathbf{x}^t, \mathbf{y}^t)}(\boldsymbol{\beta}^t)\|^2. \quad (\text{F.1})$$

By the strong Minty condition in Assumption 4.1, we have

$$\mathbb{E} [\langle V_{(\mathbf{x}^t, \mathbf{y}^t)}(\boldsymbol{\beta}^t), \boldsymbol{\beta}^t - \boldsymbol{\beta}^* \rangle] \geq \mu \mathbb{E} \|\boldsymbol{\beta}^t - \boldsymbol{\beta}^*\|^2.$$

In addition, Lemma D.1 implies that $\|V_{(\mathbf{x}^t, \mathbf{y}^t)}(\boldsymbol{\beta}^t)\|^2 \leq (d+1)R^2M^2$. Substituting these bounds into (F.1) yields

$$\frac{1}{2} \mathbb{E} \|\boldsymbol{\beta}^{t+1} - \boldsymbol{\beta}^*\|^2 \leq \frac{1}{2} (1 - 2\mu\eta^t) \mathbb{E} \|\boldsymbol{\beta}^t - \boldsymbol{\beta}^*\|^2 + \frac{1}{2} (\eta^t)^2 (d+1)R^2M^2.$$

Let $\eta^t = 1/[\mu(t+1)]$ and assume the initialization satisfies

$$\frac{1}{2} \mathbb{E} \|\boldsymbol{\beta}^0 - \boldsymbol{\beta}^*\|^2 \leq \frac{c_0(d+1)R^2M^2}{2\mu^2}$$

for some constant $c_0 > 1$. We will prove by induction that

$$\frac{1}{2} \mathbb{E} \|\boldsymbol{\beta}^t - \boldsymbol{\beta}^*\|^2 \leq \frac{c_0(d+1)R^2M^2}{2\mu^2(t+1)}, \quad t = 0, 1, \dots$$

The base case $t = 0$ holds by assumption. For the induction step, note that $\mu\eta^t = 1/(t+1) \leq 1/2$. Then,

$$\begin{aligned} \frac{1}{2}\mathbb{E}\|\boldsymbol{\beta}^{t+1} - \boldsymbol{\beta}^*\|^2 &\leq \frac{1}{2}(1 - 2\mu\eta^t)\mathbb{E}\|\boldsymbol{\beta}^t - \boldsymbol{\beta}^*\|^2 + \frac{1}{2}(\eta^t)^2(d+1)R^2M^2 \\ &\leq \frac{c_0(d+1)R^2M^2}{2\mu^2t}(1 - 2\mu\eta^t) + \frac{1}{2}(\eta^t)^2(d+1)R^2M^2 \\ &\leq \frac{c_0(d+1)R^2M^2}{2\mu^2t}\left(1 - \frac{2}{t+1}\right) + \frac{c_0(d+1)R^2M^2}{2\mu^2(t+1)^2} \\ &= \frac{c_0(d+1)R^2M^2}{2\mu^2(t+1)}\left(\frac{t-1}{t} + \frac{1}{t+1}\right) \leq \frac{c_0(d+1)R^2M^2}{2\mu^2(t+1)}. \end{aligned}$$

This completes the induction and thus the proof. \square

G Additional Experiment Results

G.1 GLM experiment

Tables 3 and 4 present additional numerical results for the finite-sample performance of VI and MLE under different parameter structures. Table 3 corresponds to the dense parameter setting $\boldsymbol{\beta}^* = d^{-1/2}(1, \dots, 1) \in \mathbb{R}^d$ as in Section 6. The results for the softplus link were already discussed in Table 2, so here we report the outcomes for the log (sanity check), clipped exponential, and Gaussian-mixture CDF links. Table 4 corresponds to the sparse parameter setting, where $\boldsymbol{\beta}^* = (2/\sqrt{5}, 1/\sqrt{5}, 0, \dots, 0) \in \mathbb{R}^d$, and summarizes the results for the softplus, clipped exponential, and Gaussian-mixture CDF links (the log link is omitted). Overall, the results under the sparse parameter setting are qualitatively similar to those under the dense parameter setting. In both cases, the VI estimator consistently outperforms MLE across most configurations, with particularly large improvements for the softplus link.

G.2 GAM experiment

We report detailed experimental settings and results for GAMs considered in Section 7. Each additive component f_j is represented using a truncated Legendre basis of degree K without the constant term, so that $f_j(0) = 0$ holds by construction. We use $d = 4$ additive components and $K = 3$ basis functions per component, with covariates independently sampled from $U[-1, 1]$. Each β_{jk} is drawn from a standard normal distribution and then normalized so that $\|\boldsymbol{\beta}\|_2 = 1$. We consider the Poisson and Bernoulli response models.

For Poisson models, we consider the canonical log link as well as softplus, clipped exponential, and Gaussian-mixture CDF links, as in the GLM experiments of Section 6. For Bernoulli models, we consider the canonical logistic link together with the non-canonical arctangent link, whose inverse is given by

$$g^{-1}(z) = \frac{1}{2} + \frac{1}{\pi} \arctan(z).$$

Figures 4 and 5 compare the recovered additive components with the ground truths, while Figures 6 and 7 report the squared error of the parameter estimates and the average L^2 errors of the additive components over iterations for the Poisson and Bernoulli models, respectively. For non-canonical links in both Poisson and Bernoulli GAMs, the VI estimator often yields slightly smoother optimization trajectories and modestly improved reconstruction of the additive components compared to MLE, although the final errors are typically of similar magnitude. These

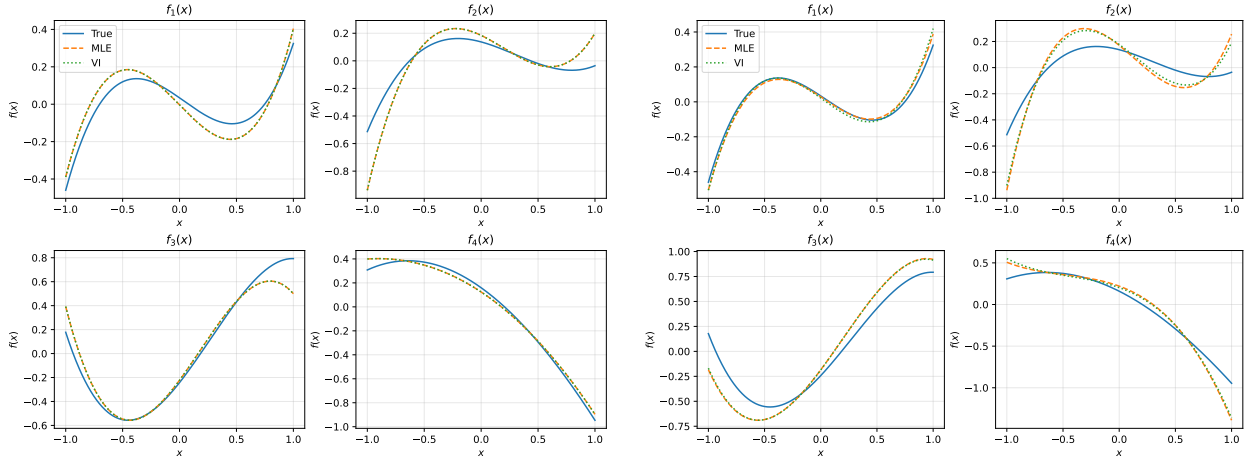
Table 3: Mean squared error of the VI estimator and MLE across link functions and iterations k with dense parameter $\beta^* = d^{-1/2}(1, \dots, 1)$. For each (Link, k, d, N) combination, the smaller error between the two estimators is highlighted in bold. The values in the brackets are standard deviations across 1000 independent repetitions.

Link, k	d	$N = 100$		$N = 200$		$N = 500$		$N = 1000$	
		VI	MLE	VI	MLE	VI	MLE	VI	MLE
log $k = 20$	10	.241 (.105)	.241 (.105)	.108 (.057)	.108 (.057)	.025 (.014)	.025 (.014)	.007 (.004)	.007 (.004)
	20	.384 (.106)	.384 (.106)	.232 (.074)	.232 (.074)	.079 (.030)	.079 (.030)	.023 (.009)	.023 (.009)
	50	.589 (.082)	.589 (.082)	.432 (.071)	.432 (.071)	.226 (.046)	.226 (.046)	.100 (.025)	.100 (.025)
	100	.719 (.061)	.719 (.061)	.586 (.062)	.586 (.062)	.379 (.049)	.379 (.049)	.221 (.032)	.221 (.032)
log $k = 50$	10	.128 (.069)	.128 (.069)	.048 (.027)	.048 (.027)	.013 (.007)	.013 (.007)	.006 (.003)	.006 (.003)
	20	.258 (.088)	.258 (.088)	.124 (.049)	.124 (.049)	.033 (.012)	.033 (.012)	.013 (.004)	.013 (.004)
	50	.485 (.080)	.485 (.080)	.307 (.063)	.307 (.063)	.120 (.030)	.120 (.030)	.045 (.011)	.045 (.011)
	100	.655 (.065)	.655 (.065)	.486 (.060)	.486 (.060)	.249 (.039)	.249 (.039)	.118 (.021)	.118 (.021)
log $k = 100$	10	.104 (.059)	.104 (.059)	.039 (.021)	.039 (.021)	.012 (.006)	.012 (.006)	.006 (.003)	.006 (.003)
	20	.221 (.078)	.221 (.078)	.101 (.039)	.101 (.039)	.028 (.010)	.028 (.010)	.012 (.004)	.012 (.004)
	50	.452 (.084)	.452 (.084)	.269 (.059)	.269 (.059)	.096 (.025)	.096 (.025)	.037 (.008)	.037 (.008)
	100	.633 (.064)	.633 (.064)	.448 (.059)	.448 (.059)	.214 (.035)	.214 (.035)	.095 (.017)	.095 (.017)
log $k = 200$	10	.096 (.053)	.096 (.053)	.037 (.020)	.037 (.020)	.012 (.006)	.012 (.006)	.006 (.003)	.006 (.003)
	20	.207 (.075)	.207 (.075)	.093 (.037)	.093 (.037)	.027 (.010)	.027 (.010)	.013 (.004)	.013 (.004)
	50	.442 (.081)	.442 (.081)	.259 (.057)	.259 (.057)	.089 (.022)	.089 (.022)	.036 (.008)	.036 (.008)
	100	.626 (.069)	.626 (.069)	.439 (.059)	.439 (.059)	.207 (.035)	.207 (.035)	.090 (.016)	.090 (.016)
clipped exp. $k = 20$	10	.593 (.068)	.595 (.066)	.484 (.054)	.488 (.051)	.342 (.042)	.346 (.036)	.241 (.030)	.245 (.024)
	20	.696 (.052)	.697 (.051)	.593 (.047)	.595 (.045)	.449 (.037)	.452 (.034)	.340 (.028)	.344 (.024)
	50	.800 (.040)	.801 (.039)	.722 (.035)	.722 (.034)	.593 (.030)	.595 (.029)	.484 (.024)	.486 (.023)
	100	.865 (.027)	.865 (.027)	.802 (.026)	.803 (.025)	.693 (.024)	.694 (.023)	.594 (.021)	.596 (.020)
clipped exp. $k = 50$	10	.444 (.084)	.456 (.076)	.334 (.066)	.344 (.056)	.201 (.048)	.208 (.036)	.125 (.033)	.128 (.022)
	20	.571 (.074)	.580 (.069)	.447 (.061)	.457 (.055)	.297 (.044)	.306 (.037)	.199 (.032)	.206 (.025)
	50	.724 (.055)	.729 (.051)	.608 (.046)	.616 (.042)	.448 (.038)	.458 (.034)	.332 (.031)	.342 (.026)
	100	.814 (.039)	.818 (.036)	.722 (.038)	.727 (.035)	.569 (.033)	.578 (.030)	.450 (.026)	.459 (.024)
clipped exp. $k = 100$	10	.388 (.090)	.403 (.081)	.273 (.068)	.285 (.057)	.156 (.048)	.161 (.034)	.089 (.033)	.090 (.021)
	20	.519 (.080)	.532 (.072)	.394 (.065)	.409 (.057)	.239 (.044)	.251 (.037)	.154 (.033)	.160 (.024)
	50	.691 (.060)	.698 (.055)	.566 (.057)	.578 (.052)	.392 (.041)	.406 (.036)	.274 (.032)	.287 (.026)
	100	.803 (.047)	.804 (.043)	.691 (.043)	.698 (.040)	.519 (.034)	.532 (.031)	.390 (.029)	.404 (.025)
clipped exp. $k = 200$	10	.377 (.094)	.393 (.083)	.255 (.070)	.270 (.058)	.141 (.046)	.145 (.033)	.080 (.032)	.080 (.020)
	20	.502 (.084)	.516 (.075)	.375 (.068)	.391 (.058)	.228 (.047)	.239 (.038)	.142 (.034)	.147 (.024)
	50	.685 (.066)	.692 (.060)	.547 (.055)	.560 (.050)	.375 (.042)	.391 (.037)	.259 (.033)	.272 (.027)
	100	.800 (.048)	.799 (.043)	.680 (.046)	.688 (.041)	.507 (.038)	.521 (.034)	.376 (.030)	.391 (.026)
GMM CDF $k = 20$	10	.167 (.061)	.459 (.094)	.076 (.030)	.271 (.069)	.023 (.010)	.074 (.026)	.010 (.004)	.017 (.007)
	20	.302 (.070)	.610 (.070)	.166 (.043)	.456 (.068)	.057 (.017)	.209 (.043)	.022 (.007)	.073 (.017)
	50	.513 (.067)	.754 (.045)	.348 (.050)	.648 (.044)	.164 (.026)	.452 (.043)	.076 (.013)	.267 (.033)
	100	.663 (.053)	.827 (.031)	.511 (.048)	.753 (.032)	.299 (.031)	.609 (.032)	.165 (.019)	.451 (.029)
GMM CDF $k = 50$	10	.103 (.045)	.200 (.079)	.049 (.023)	.079 (.036)	.019 (.009)	.017 (.008)	.010 (.004)	.007 (.003)
	20	.210 (.066)	.371 (.086)	.105 (.035)	.201 (.053)	.039 (.013)	.055 (.018)	.019 (.006)	.017 (.005)
	50	.435 (.074)	.588 (.068)	.260 (.051)	.426 (.059)	.104 (.022)	.199 (.035)	.049 (.010)	.079 (.015)
	100	.624 (.063)	.715 (.048)	.435 (.055)	.586 (.050)	.213 (.028)	.370 (.038)	.105 (.015)	.199 (.025)
GMM CDF $k = 100$	10	.098 (.046)	.145 (.066)	.048 (.023)	.052 (.025)	.019 (.009)	.014 (.006)	.010 (.005)	.007 (.003)
	20	.200 (.065)	.297 (.082)	.100 (.033)	.143 (.045)	.039 (.013)	.037 (.013)	.019 (.006)	.014 (.005)
	50	.424 (.079)	.525 (.072)	.240 (.049)	.344 (.058)	.099 (.021)	.141 (.028)	.048 (.010)	.051 (.011)
	100	.625 (.070)	.671 (.056)	.419 (.056)	.520 (.051)	.197 (.027)	.292 (.036)	.098 (.015)	.140 (.020)
GMM CDF $k = 200$	10	.099 (.050)	.131 (.067)	.049 (.023)	.047 (.023)	.020 (.010)	.014 (.007)	.010 (.004)	.007 (.003)
	20	.196 (.066)	.273 (.079)	.097 (.032)	.127 (.042)	.038 (.013)	.034 (.012)	.019 (.006)	.014 (.004)
	50	.421 (.083)	.507 (.077)	.241 (.049)	.328 (.057)	.098 (.020)	.125 (.027)	.049 (.010)	.047 (.010)
	100	.629 (.075)	.660 (.057)	.421 (.056)	.503 (.052)	.195 (.029)	.271 (.035)	.097 (.015)	.127 (.020)

Table 4: Mean squared error of the VI estimator and MLE across link functions and iterations k with sparse parameter $\beta^* = (2/\sqrt{5}, 1/\sqrt{5}, 0, \dots, 0)$.

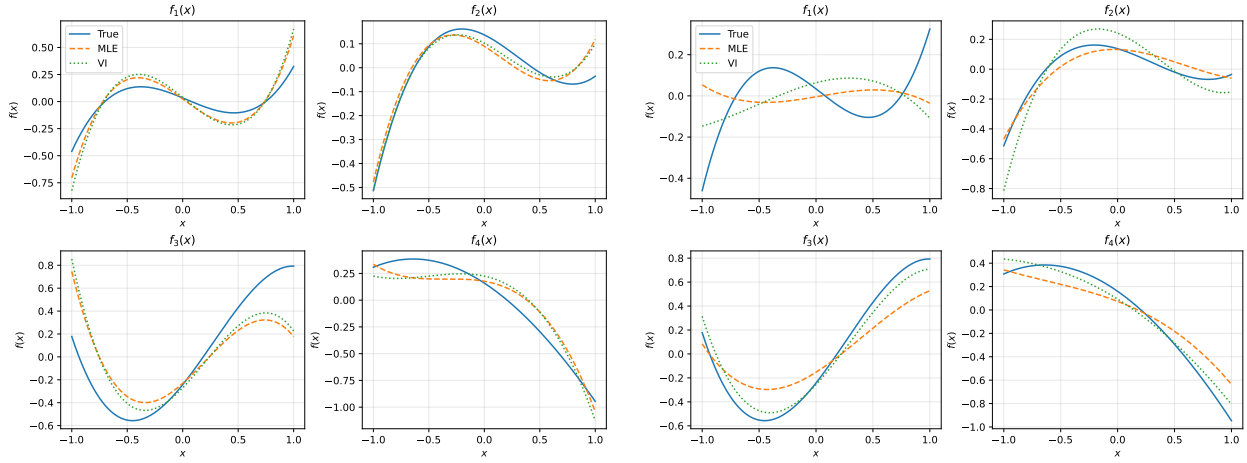
Link, k	d	$N = 100$		$N = 200$		$N = 500$		$N = 1000$	
		VI	MLE	VI	MLE	VI	MLE	VI	MLE
softplus $k = 20$	10	.632 (.078)	.717 (.061)	.513 (.069)	.619 (.055)	.339 (.054)	.464 (.046)	.216 (.037)	.342 (.034)
	20	.731 (.064)	.795 (.049)	.625 (.058)	.711 (.046)	.463 (.047)	.577 (.038)	.334 (.036)	.461 (.030)
	50	.832 (.043)	.872 (.032)	.757 (.042)	.815 (.032)	.631 (.037)	.716 (.028)	.508 (.030)	.615 (.024)
	100	.882 (.031)	.909 (.023)	.823 (.029)	.865 (.022)	.726 (.028)	.791 (.021)	.626 (.027)	.712 (.021)
softplus $k = 50$	10	.469 (.106)	.570 (.088)	.341 (.080)	.455 (.069)	.159 (.048)	.268 (.048)	.078 (.028)	.161 (.032)
	20	.585 (.082)	.668 (.066)	.459 (.078)	.562 (.066)	.276 (.053)	.393 (.048)	.164 (.033)	.273 (.033)
	50	.748 (.058)	.798 (.046)	.637 (.062)	.710 (.050)	.460 (.052)	.563 (.043)	.324 (.034)	.439 (.030)
	100	.827 (.046)	.858 (.036)	.741 (.047)	.792 (.037)	.596 (.039)	.677 (.032)	.465 (.032)	.567 (.027)
softplus $k = 100$	10	.400 (.117)	.498 (.102)	.258 (.080)	.365 (.075)	.115 (.042)	.201 (.046)	.048 (.021)	.105 (.027)
	20	.535 (.103)	.617 (.085)	.401 (.083)	.501 (.070)	.215 (.051)	.321 (.049)	.116 (.035)	.204 (.038)
	50	.717 (.064)	.766 (.050)	.584 (.063)	.659 (.052)	.397 (.048)	.498 (.041)	.258 (.037)	.365 (.034)
	100	.818 (.053)	.843 (.042)	.706 (.053)	.756 (.043)	.539 (.042)	.621 (.035)	.394 (.031)	.495 (.027)
softplus $k = 200$	10	.378 (.111)	.476 (.099)	.232 (.079)	.335 (.077)	.100 (.037)	.179 (.043)	.045 (.019)	.093 (.025)
	20	.527 (.106)	.607 (.089)	.382 (.080)	.479 (.071)	.200 (.051)	.300 (.050)	.102 (.029)	.182 (.032)
	50	.707 (.075)	.754 (.061)	.574 (.069)	.647 (.057)	.375 (.049)	.475 (.043)	.241 (.034)	.344 (.032)
	100	.817 (.057)	.839 (.045)	.701 (.058)	.750 (.046)	.521 (.045)	.603 (.038)	.376 (.036)	.475 (.032)
clipped exp. $k = 20$	10	.596 (.064)	.598 (.062)	.487 (.057)	.491 (.054)	.339 (.039)	.343 (.035)	.241 (.030)	.244 (.024)
	20	.694 (.053)	.695 (.051)	.595 (.042)	.597 (.040)	.444 (.038)	.448 (.035)	.341 (.027)	.345 (.024)
	50	.800 (.037)	.801 (.036)	.721 (.036)	.722 (.035)	.590 (.028)	.592 (.027)	.485 (.025)	.488 (.023)
	100	.867 (.024)	.868 (.024)	.799 (.025)	.799 (.025)	.692 (.025)	.693 (.024)	.595 (.019)	.597 (.019)
clipped exp. $k = 50$	10	.447 (.085)	.457 (.077)	.325 (.061)	.337 (.051)	.203 (.045)	.210 (.034)	.126 (.036)	.130 (.023)
	20	.572 (.067)	.581 (.061)	.445 (.063)	.459 (.056)	.298 (.045)	.308 (.037)	.199 (.031)	.206 (.024)
	50	.720 (.058)	.726 (.054)	.611 (.048)	.619 (.045)	.445 (.041)	.455 (.036)	.332 (.027)	.342 (.023)
	100	.813 (.040)	.816 (.037)	.724 (.041)	.729 (.038)	.566 (.032)	.575 (.029)	.446 (.027)	.457 (.024)
clipped exp. $k = 100$	10	.390 (.093)	.406 (.083)	.275 (.068)	.287 (.055)	.156 (.045)	.164 (.033)	.091 (.036)	.091 (.025)
	20	.520 (.082)	.533 (.074)	.391 (.062)	.407 (.056)	.241 (.049)	.251 (.038)	.154 (.034)	.159 (.025)
	50	.684 (.054)	.692 (.051)	.567 (.052)	.578 (.048)	.389 (.043)	.404 (.037)	.278 (.032)	.290 (.027)
	100	.799 (.046)	.801 (.041)	.688 (.045)	.696 (.041)	.521 (.036)	.533 (.032)	.393 (.030)	.407 (.026)
clipped exp. $k = 200$	10	.384 (.085)	.396 (.076)	.259 (.072)	.273 (.061)	.142 (.046)	.148 (.035)	.078 (.030)	.080 (.019)
	20	.506 (.086)	.520 (.078)	.368 (.065)	.386 (.057)	.230 (.048)	.239 (.038)	.142 (.034)	.149 (.024)
	50	.676 (.063)	.683 (.059)	.550 (.054)	.562 (.049)	.373 (.040)	.389 (.034)	.265 (.032)	.276 (.026)
	100	.798 (.054)	.798 (.048)	.682 (.047)	.690 (.043)	.504 (.037)	.518 (.033)	.374 (.031)	.390 (.027)
GMM CDF $k = 20$	10	.171 (.066)	.467 (.097)	.075 (.027)	.273 (.068)	.022 (.010)	.073 (.023)	.009 (.004)	.017 (.007)
	20	.304 (.072)	.608 (.070)	.164 (.041)	.456 (.065)	.057 (.017)	.208 (.038)	.022 (.007)	.074 (.016)
	50	.512 (.066)	.756 (.043)	.348 (.052)	.647 (.048)	.166 (.026)	.455 (.040)	.075 (.014)	.266 (.031)
	100	.666 (.051)	.828 (.030)	.515 (.047)	.755 (.034)	.302 (.031)	.611 (.031)	.165 (.019)	.453 (.031)
GMM CDF $k = 50$	10	.107 (.054)	.201 (.086)	.050 (.023)	.084 (.037)	.019 (.009)	.017 (.008)	.009 (.004)	.007 (.003)
	20	.221 (.072)	.384 (.093)	.105 (.035)	.199 (.053)	.039 (.013)	.054 (.018)	.019 (.006)	.017 (.005)
	50	.421 (.079)	.577 (.071)	.259 (.050)	.429 (.058)	.104 (.019)	.199 (.033)	.048 (.009)	.076 (.014)
	100	.627 (.070)	.719 (.053)	.433 (.057)	.585 (.050)	.212 (.027)	.370 (.035)	.104 (.015)	.199 (.023)
GMM CDF $k = 100$	10	.095 (.046)	.134 (.063)	.051 (.026)	.055 (.027)	.019 (.008)	.014 (.006)	.010 (.005)	.006 (.003)
	20	.201 (.063)	.301 (.087)	.098 (.033)	.143 (.050)	.038 (.012)	.037 (.012)	.019 (.006)	.014 (.004)
	50	.421 (.081)	.522 (.071)	.244 (.049)	.347 (.063)	.098 (.020)	.141 (.029)	.049 (.011)	.052 (.012)
	100	.623 (.068)	.670 (.054)	.425 (.052)	.522 (.049)	.199 (.032)	.288 (.037)	.100 (.015)	.142 (.021)
GMM CDF $k = 200$	10	.096 (.047)	.128 (.064)	.051 (.024)	.048 (.023)	.021 (.010)	.014 (.007)	.009 (.004)	.007 (.003)
	20	.192 (.060)	.277 (.082)	.095 (.033)	.130 (.041)	.039 (.013)	.033 (.011)	.020 (.006)	.014 (.005)
	50	.415 (.077)	.499 (.071)	.245 (.050)	.331 (.063)	.099 (.020)	.131 (.026)	.048 (.010)	.046 (.010)
	100	.629 (.076)	.659 (.059)	.426 (.061)	.506 (.056)	.196 (.031)	.273 (.037)	.098 (.015)	.125 (.019)

experiments illustrate that the proposed VI framework extends naturally to GAMs through basis representations and remains numerically stable in additive models beyond linear predictors.



(a) log

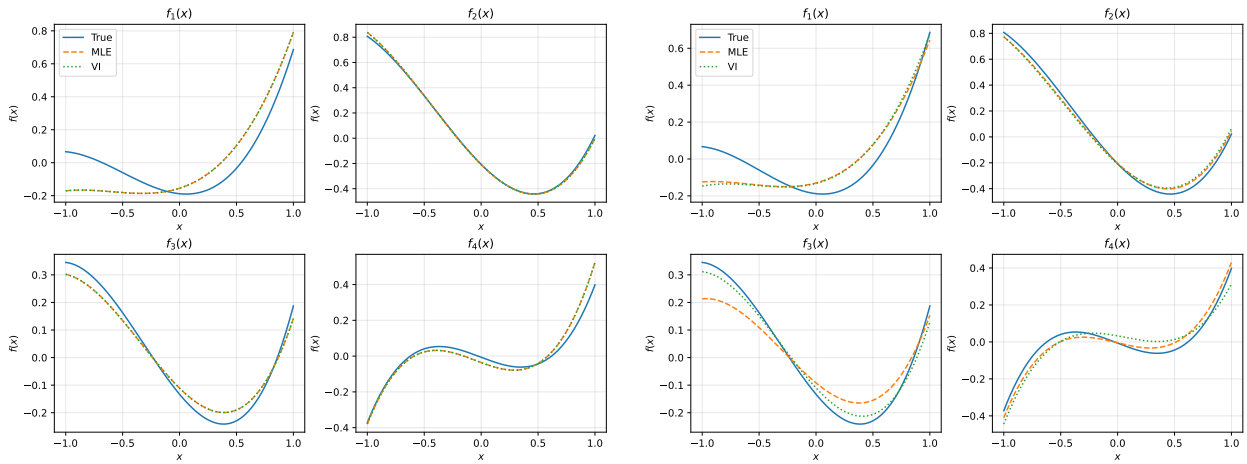
(b) softplus



(c) clipped exp.

(d) GMM CDF

Figure 4: Reconstruction of additive components in GAMs under Poisson distribution.



(a) logistic

(b) arctangent

Figure 5: Reconstruction of additive components in GAMs under Bernoulli distribution.

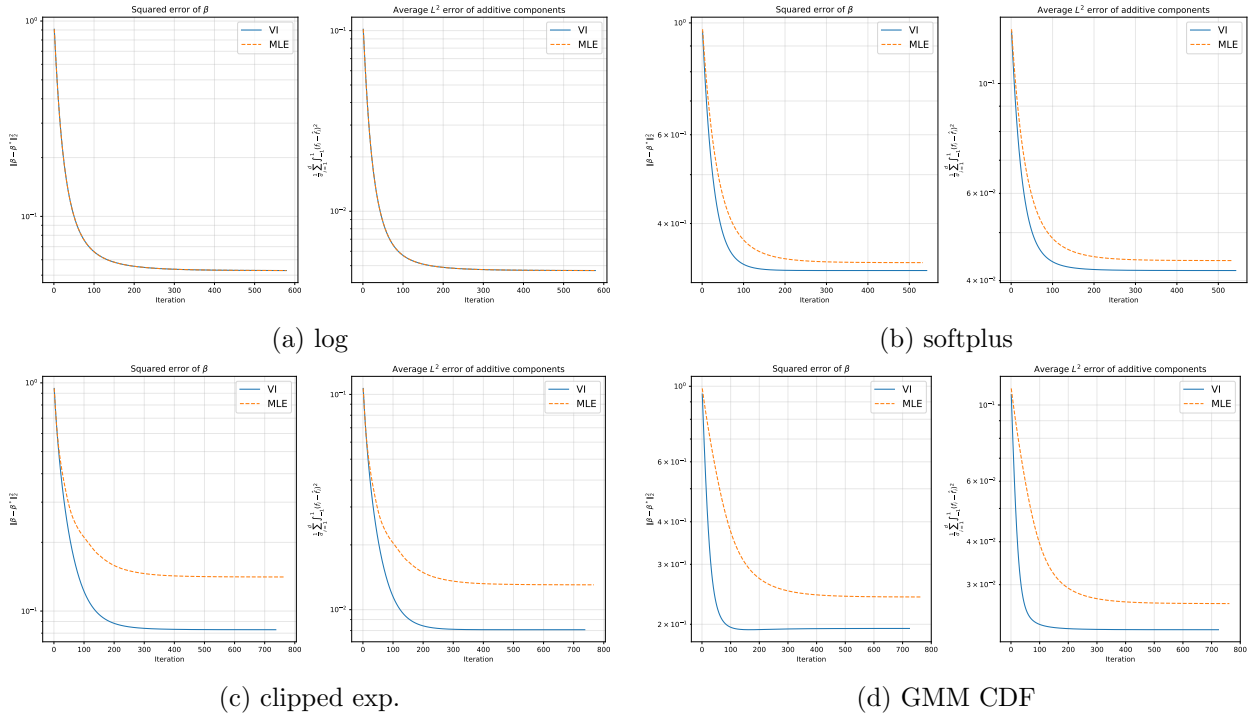


Figure 6: Squared error of parameter estimates and the average L^2 error of the additive components (Poisson response)

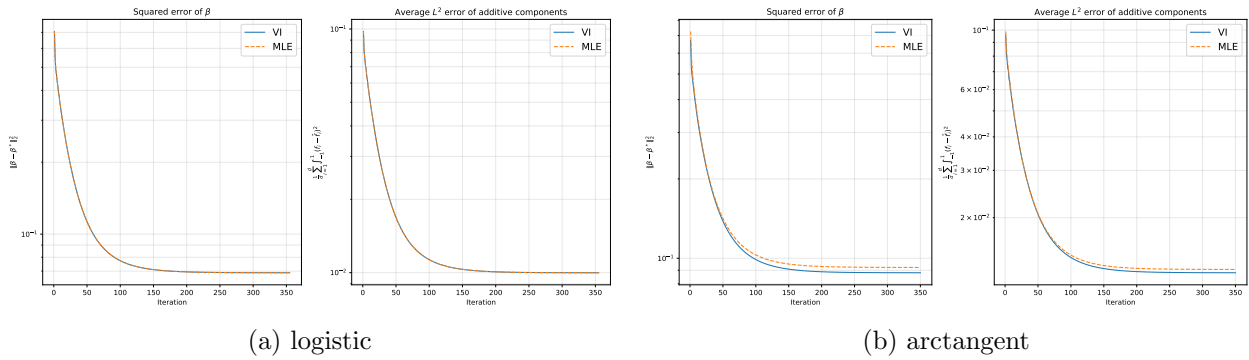


Figure 7: Squared error of parameter estimates and the average L^2 error of the additive components (Bernoulli response)